

**Forschungszentrum Karlsruhe**  
Technik und Umwelt

**Wissenschaftliche Berichte**  
FZKA 6355

# **Deflagration to Detonation Transition Experiments with Hydrogen-Air Mixtures in Shock Tube and Obstacle Array Geometries**

**A. Veser, W. Breitung, G. Engel, G. Stern,  
A. Kotchourko**

**Institut für Kern- und Energietechnik  
Projekt Nukleare Sicherheitsforschung**

**Dezember 1999**

---



# **Forschungszentrum Karlsruhe**

Technik und Umwelt

Wissenschaftliche Berichte

FZKA 6355

## **Deflagration to Detonation Transition Experiments with Hydrogen-Air Mixtures in Shock Tube and Obstacle Array Geometries**

A. Vesper, W. Breitung, G. Engel, G. Stern, A. Kotchourko

Institut für Kern- und Energietechnik

Projekt Nukleare Sicherheitsforschung

**Als Manuskript gedruckt**  
**Für diesen Bericht behalten wir uns alle Rechte vor**  
**Forschungszentrum Karlsruhe GmbH**  
**Postfach 3640, 76021 Karlsruhe**  
**Mitglied der Hermann von Helmholtz-Gemeinschaft**  
**Deutscher Forschungszentren (HGF)**  
**ISSN 0947-8620**

## Abstract

### Deflagration to Detonation Transition Experiments with Hydrogen- Air Mixtures in Shock Tube and Obstacle Array Geometries

The objectives of this work were

1. to provide integral experimental data for development of physical models and verification of numerical tools,
2. to investigate the statistical nature of DDT for well defined initial and boundary conditions,
3. to measure typical DDT loads in lean hydrogen-air mixtures.

Different DDT mechanisms were investigated in three test configurations:

- idealised mode A (shock wave focussing in a 3-d reflector)
- prototypic mode A (focussing of flame precursor wave in a 3-d reflector)
- prototypic mode B (accelerating flame in obstacle array).

For DDT by idealised mode A critical Mach numbers were determined for the incident shock as function of the H<sub>2</sub> concentration. At this critical Mach number the ignition regime changes from slow/weak (= deflagration) to strong/fast (= detonation). Very good reproducibility of individual tests and consistence of the whole data base in terms of ignition modes was observed. The detailed processes in idealised mode A DDT tests are highly mechanistic and seem to be governed by the temperature dependent reaction kinetics.

Prototypic DDT mode A from the precursor wave of an accelerating flame was detected in the FZK-tube at > 16.5% H<sub>2</sub> in air, with a blockage ratio of 60%. At smaller hydrogen concentrations the precursor shock caused only a mild ignition (=deflagration) in the reflector. The tests have clearly proven the significance of DDT mode A in obstructed geometries: a flame which accelerates in a certain part of a complex installation to near sonic velocities emits pressure waves which can trigger a DDT in a distant part of the enclosure, especially if H<sub>2</sub> enrichments should be present in reflecting corners, e.g. caused by stratification.

DDT mode B was observed in the fully obstructed tube for > 13.5% H<sub>2</sub> at 30% BR and for > 15% H<sub>2</sub> at 45% BR. With 60% BR no DDT occurred for ≤ 15% H<sub>2</sub> (p<sub>0</sub>=1bar). The occurrence of DDT could be clearly identified by three criteria, namely pressure amplitude, wave speed, and coupling of pressure and reaction front.

Pressures developing due to DDT in lean H<sub>2</sub>-air mixtures were measured. The highest pressures are generated during the initial ignition phase in the reflector when the reaction starts from a highly pre-compressed state.

The tests have resulted in new data on DDT mechanisms which can be used for model development and verification with increasing complexity. The simplest case are the idealised mode A experiments, which requires only simulation of the

compressible flow and the  $H_2-O_2$  reaction but not of turbulence. Numerical models should be first verified on these tests.

## Zusammenfassung

### Experimente zu Deflagrations-Detonations-Übergängen (DDT) bei Wasserstoff-Luft-Gemischen in Stoßrohr- und Hindernisstreckengeometrie

Ziel der Arbeiten war

- integrale Meßdaten für die Entwicklung physikalischer Modelle und Verifikation numerischer Programme bereitzustellen,
- die statistische Natur von DDT- Vorgängen bei gut definierten Anfangs- und Randbedingungen zu untersuchen,
- typische DDT- Lasten in mageren H<sub>2</sub>- Luft- Gemischen zu messen.

Verschiedene DDT- Mechanismen wurden in drei unterschiedlichen Meßanordnungen untersucht:

- Idealisierter DDT- Mode A, d.h. Fokussierung von Stoßwellen in einem 3D-Reflektor,
- prototypischer Mode A, d.h. Fokussierung einer flammenerzeugten Druckwelle in einem 3D- Reflektor,
- prototypischer Mode B, d.h. DDT durch eine beschleunigende Flamme in einer Hindernisstrecke.

Für DDT durch den idealisierten Mode A wurden kritische Machzahlen als Funktion der H<sub>2</sub>- Konzentration bestimmt. Bei dieser kritischen Machzahl wechselt der Zündvorgang von langsam / schwach (= Deflagration) in schnell / stark (= Detonation). Es zeigt sich eine sehr gute Reproduzierbarkeit der einzelnen Versuche und Konsistenz der Daten untereinander. Die Detailvorgänge bei der Fokussierung von Stoßwellen in diesen Versuchen verlaufen weitgehend mechanistisch ohne nennenswerte statistische Streuung. Sie scheinen von der temperaturabhängigen Reaktionskinetik des hochkomprimierten Gases (hier H<sub>2</sub>-Luft) bestimmt zu sein.

Der prototypische DDT-Mode A , verursacht durch eine flammenerzeugte Druckwelle, trat im FZK- Versuchsrohr bei > 16,5% H<sub>2</sub> auf (12m lang, 35 cm Durchmesser, Hindernisse mit 60% Versperrungsgrad). Bei geringeren H<sub>2</sub>-Konzentrationen verursachte die Druckwelle nur eine milde deflagrative Zündung im Fokus des konischen Reflektors. Die Versuche haben die Bedeutung dieses DDT- Modes bei versperrten Geometrien gezeigt: Eine Flamme, die in einem mit Strömungshindernissen teilweise versperrten Teil einer komplexen technischen Anlage auf hohe Geschwindigkeiten beschleunigt (z.B. 500-800 m/s bei H<sub>2</sub>-Luft), sendet Druckwellen aus, die in einem entfernten Teil der Umschließung ein DDT- Ereignis verursachen können, insbesondere wenn dort lokale H<sub>2</sub>- Anreicherungen wie z.B. durch Stratifikation vorliegen.

DDT Mode B wurde im FZK Rohr mit 30% Versperrungsgrad für  $> 13,5\%$   $H_2$  in Luft beobachtet. Bei 45% Versperrungsgrad trat DDT nur auf für  $> 16,5\%$   $H_2$ . Bei 60% Versperrungsgrad ergab sich kein Mode- B- DDT für  $\leq 15\%$   $H_2$ . Alle Versuche wurden mit einem Anfangsdruck von 1 bar durchgeführt. Das Auftreten von DDT konnte durch drei Kriterien klar identifiziert werden, nämlich durch die gemessene Druckamplituden, die Geschwindigkeit der Reaktionsfront, und die enge Kopplung zwischen Druck- und Reaktionsfront.

Die Druckentwicklung bei DDT Vorgängen in mageren  $H_2$ - Luft- Gemischen wurden systematisch ausgewertet. Die höchsten lokalen Drücke entstehen während der anfänglichen Zündphase im Reflektor, wenn die chemischen Reaktion des hochkomprimierten und erhitzten Gases einsetzt.

Die Versuche haben eine neue umfangreiche Datenbasis für DDT- Vorgänge in mageren  $H_2$ - Luft- Gemischen auf relativ großer Skala geliefert. Die Ergebnisse dienen der Modellentwicklung und- verifikation mit zunehmender Komplexität. Der einfachste Fall sind die idealisierten Mode- A- Experimente bei denen nur die kompressible Strömung und die  $H_2$ -  $O_2$  Reaktionskinetik simuliert werden müssen, nicht aber Turbulenz. Numerische Modellentwicklungen sollten daher zuerst an diesen Daten überprüft werden.

## CONTENTS

<b>1 Introduction</b>	<b>1</b>
1.1 Relevance of FA and DDT in severe accidents	1
1.2 Basic physical processes	2
1.3 Objectives	3
<b>2 Experimental investigations</b>	<b>4</b>
2.1 Results of idealized mode A-DDT experiments	7
2.2 Results of prototypic mode B-DDT experiments	30
2.3 Results of mode B-DDT experiments	37
<b>3 Numerical simulation of DDT</b>	<b>45</b>

# 1. Introduction

## 1.1 Relevance of FA and DDT in severe accidents.

The relevance of FA and DDT processes in postulated severe accidents arises from theoretical estimates and large scale experiments.

The assumption that 100 % of the fuel cladding Zircalloy oxidize (but not the other in-vessel Zr or steel structures) and that the generated hydrogen is distributed homogeneously in the available containment volume, leads in American plant designs to dry hydrogen concentrations between 12 and 21 % [1]. For operating and future European PWR designs with a large dry containment the same assumptions lead to dry H<sub>2</sub> concentrations between 17 and 20 % [2]. Typical steam concentrations are 20 – 70 %, depending on the accident scenario. These conditions define the "global distribution" area in Fig. 1. Since nuclear power plant (NPP) containments are highly complex multicompartiment structures, H<sub>2</sub> gradients can generally develop in certain space and time regions. The inhomogeneity of the hydrogen distribution depends mainly on details of the H<sub>2</sub>-source (location, release rate), the containment design and the efficiency of natural convection processes. 3-d distribution calculations for German 1300 MWe PWR's have often shown gas compositions in the "local distribution" area in Fig. 1.

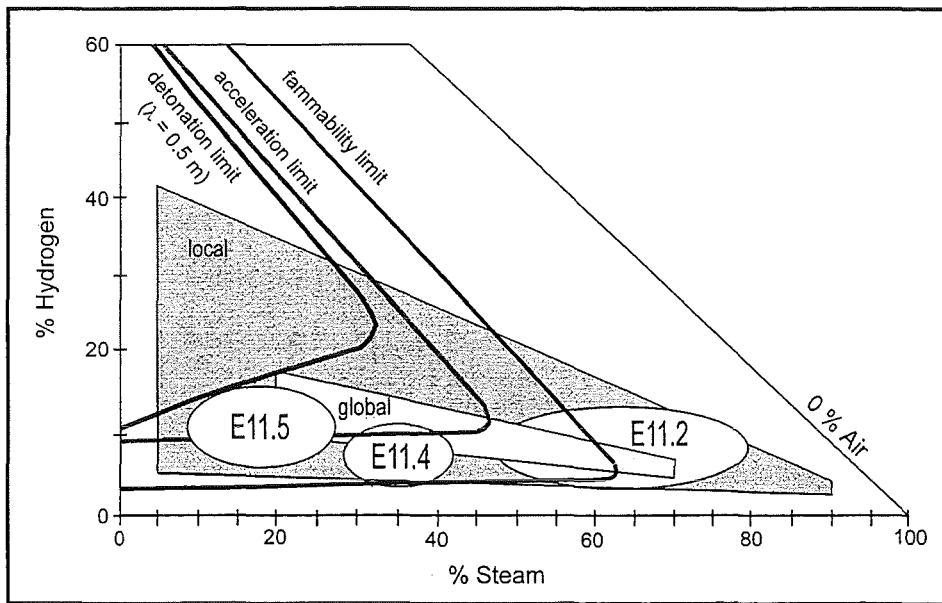


**Fig.1.**Theoretical estimates and large scale HDR E-11 distribution tests demonstrate the possibility of flame acceleration and DDT processes in severe accidents.

Hydrogen distribution under severe accident conditions was extensively investigated on full reactor scale in the HDR-E11 test serie, using He-gas as H<sub>2</sub> simulant [3]. Typical measured H<sub>2</sub> (He)-steam concentrations are included in Fig. 1 for HDR tests simulating different accident sequences.

Fig. 1 also shows estimates for limits of flammability, flame acceleration and DDT on large scale. Comparison with the above described fields of possible gas compositions clearly shows that flame acceleration (FA) and DDT are relevant for severe accident studies. These fast combustion modes appear possible on local and even global scale, depending on details of the hydrogen source. It is important to note that also the steam concentration in the containment has a large effect on the combustion mode. The steam concentration is mainly governed by the balance between steam release rate and steam condensation rate, which in turn depends on the size and surface temperature of the internal containment structures. Relatively dry or wet containment atmospheres can develop in different accident sequences, as e.g. demonstrated by the HDR distribution tests E11.5 and E11.2, respectively. Flame acceleration and DDT become a major concern in dry or medium-dry scenarios (E11.5, E11.4)

## 1.2 Basic physical processes

If severe accidents should lead to mixtures inside the detonation limits shown in Fig.1, two classes of detonation initiation can be distinguished in principle:

- direct strong initiation by an external energy source,
- indirect initiation with a weak ignition, followed by a self-induced flame acceleration and DDT.

In the first case the energy necessary to establish a self-sustaining stable detonation front wave system is provided by the external source, e.g. a spark or high explosive. In the second case the initiation energy is provided by the combustible mixture itself. Different modes have been observed for the indirect detonation initiation, it can be induced e.g. by flame acceleration along tubes or channels, turbulent jets and turbulence generating fans.

In severe accident environments the direct initiation by an external energy source seems less likely than the indirect mode, because the necessary initiation energies are much larger than those for a weak ignition. The measured orders of magnitude for direct initiation in free clouds are 10 – 1000 kJ for H<sub>2</sub>-air mixtures with equivalence ratios from 0.75 to 0.5 [4], whereas only mJ are required to trigger a weak ignition in H<sub>2</sub>-air mixtures. The only potential ignition source for a direct initiation may be a high-voltage spark or arc in a well confined geometry. Many more possibilities exist for weak ignitions. It has been suspected that the spontaneous burn in the TMI-2 accident, which led to the only significant containment load (3 bar), was initiated by a ringing telephone.

The processes following a weak ignition in a sensible combustible mixture enclosed by a complicated 3-d structure with internal flow obstacles involve extremely complex interactions between turbulent flow and chemistry. From an global point of view chemical energy is converted and concentrated to high mechanical energy densities which in turn trigger large chemical reaction rates through high temperatures. The simulation of these processes generally requires computation of unsteady, turbulent,

and compressible reactive flow problems in multidimensional geometries with high spatial resolution.

The significance of flame acceleration and DDT processes for reactor safety is due to the fact that these fast combustion modes can be extremely destructive. They have the highest damage potential for internal containment structures, safety systems which are required for safe termination of the accident (sprays, recombiners), and the outer containment shell which is the last barrier against radioactive release to the environment.

The concern about the outer containment shell is not only connected to its ultimate barrier function, but also due to its complicated structural behaviour. All modern containment buildings are a complex composite of different structural elements, including an undisturbed shell, personal and material locks and hatches of different sizes and design, as well as penetrations for electrical cables and pipes. This system has been qualified for a certain global and static design pressure which is generally related to the maximum blow-down pressure from a break of the primary coolant line.

However, in a severe accident, which is not part of the licensing process in existing plants, flame acceleration and DDT may become possible. In this case new containment load classes would arise, namely high local or even global dynamic loads. The structural behaviour of containment components under such dynamic pressure and impulse loads is complicated and difficult to evaluate. An effective way to protect the containment integrity even for the case of beyond-design accidents, is therefore to control the hydrogen behaviour in such a way that the possibility for flame acceleration and DDT is decreased or even excluded. It is clear that this improvement of public and environmental protection against the consequences of severe accidents, requires a detailed understanding of FA and DDT.

### **1.3 Objectives**

In complex technical installations pressure waves can be focussed and amplified in a large variety of multidimensional reflecting geometries, e.g. 2-d wedges or 3-d corners. In the presence of sufficiently reactive gases the reflection process can lead to a deflagrative or detonative ignition of the mixture. The detonation-like ignition in multidimensional reflectors can occur much easier than with flat reflecting surfaces because significantly higher local pressures and temperatures are reached during the initial gas compression phase. A limited number of experiments have been made so far on small scale [5, overview in 6] showing a dependence of the limit between the weak and strong ignition regime on the geometrical scale of the facility.

For scaling to reactor typical dimensions a detailed understanding of the interaction between compressible flow, chemistry and turbulence is necessary. The goal of the described experiments is to provide insight into the dependence of various mechanisms of detonation formation on global parameters such as H<sub>2</sub>- air mixture composition, thermodynamic state, obstacle configuration and geometrical confinement on large scale. Pure shock induced detonation ignition as well as detonations due to accelerating flames are investigated.

The three main objectives of the work are

- To provide integral experimental data for the development of physical models and verification of numerical tools,
- to investigate the statistical nature of DDT for well defined initial and boundary conditions, and
- to measure typical DDT pressure loads from lean H<sub>2</sub>- air mixtures.

## 2. Experimental investigations

Three different series of DDT experiments have been performed in the FZK combustion research facility. Fig.2 shows the FZK-12m-tube, which has an inner diameter of 0.35 m. The three main experimental configurations are given in Figure 3. Mode A refers to DDT processes far in front of the flame, mode B refers to DDT in or near the turbulent flame. The three test series can be summarised as follows.

### a) Shock tube with conus (idealised mode A)

The tube was divided by a membrane into a low pressure section (length 9 m) and a high pressure section (length 3 m). The experiments were carried out with a conical reflector at the end of the low pressure section to focus the pressure wave and to reach self-ignition temperatures. The main idea behind this experiment design is the observation that in many tests with fast combustion modes, DDT events are apparently triggered by waves reflected in corners or other converging multidimensional parts of the test enclosure. The conus is used to produce local hot spots in the combustible gas as they generally develop from the interaction of a pressure wave with a complex multidimensional target.

After evacuating both sections, the low pressure section was filled up to the desired initial pressure with a defined hydrogen/air mixture. The parameters varied during the experiments were the initial pressure (0.5-1.5 bar) and the composition of the hydrogen/air mixture (9-30 % H<sub>2</sub>). The high pressure section was filled with helium up to membrane failure. To detect DDT processes pressure transducers, photodiodes, and film thermocouples were located along the tube. Ionisation gauges were installed in and near the conus.

### b) Partially obstructed tube with conus (prototypic mode A)

In this case a part of the tube was equipped with an array of ring obstacles blocking 30 % of the flow cross section (BR=30%) over a length of 5-6 m to accelerate the flame to a high velocity. The tube also contained a conus to focus the precursor shock wave. It was evacuated and then filled with a defined hydrogen/air mixture (9-20 % H<sub>2</sub>) to the initial pressure (1 bar). The mixture was ignited with a glow plug. Pressure transducers, ionisation gauges, photodiodes and film thermocouples were used to locate the expected DDT events

### c) Fully obstructed tube (prototypic mode B)

The combustion tube was equipped with an array of ring obstacles (BR = 60 %) over its full length of 12 m. The evacuated tube was filled with a defined hydrogen/air mixture (9-20 % H<sub>2</sub>) up to the initial pressure (0.5-2.0 bar) and then ignited with a glow plug. To observe the combustion process pressure transducers, photodiodes and film thermocouples were located along the tube.

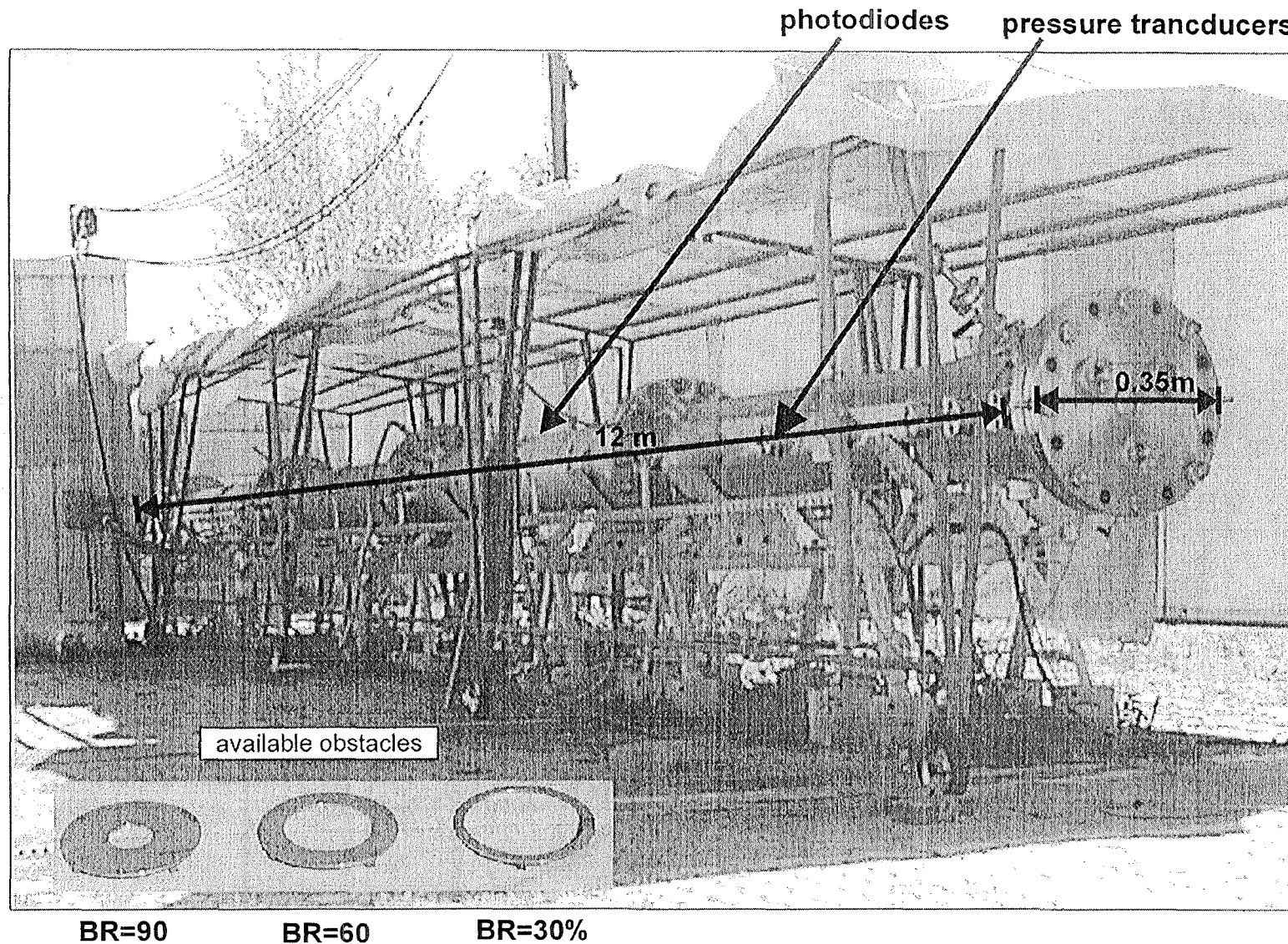
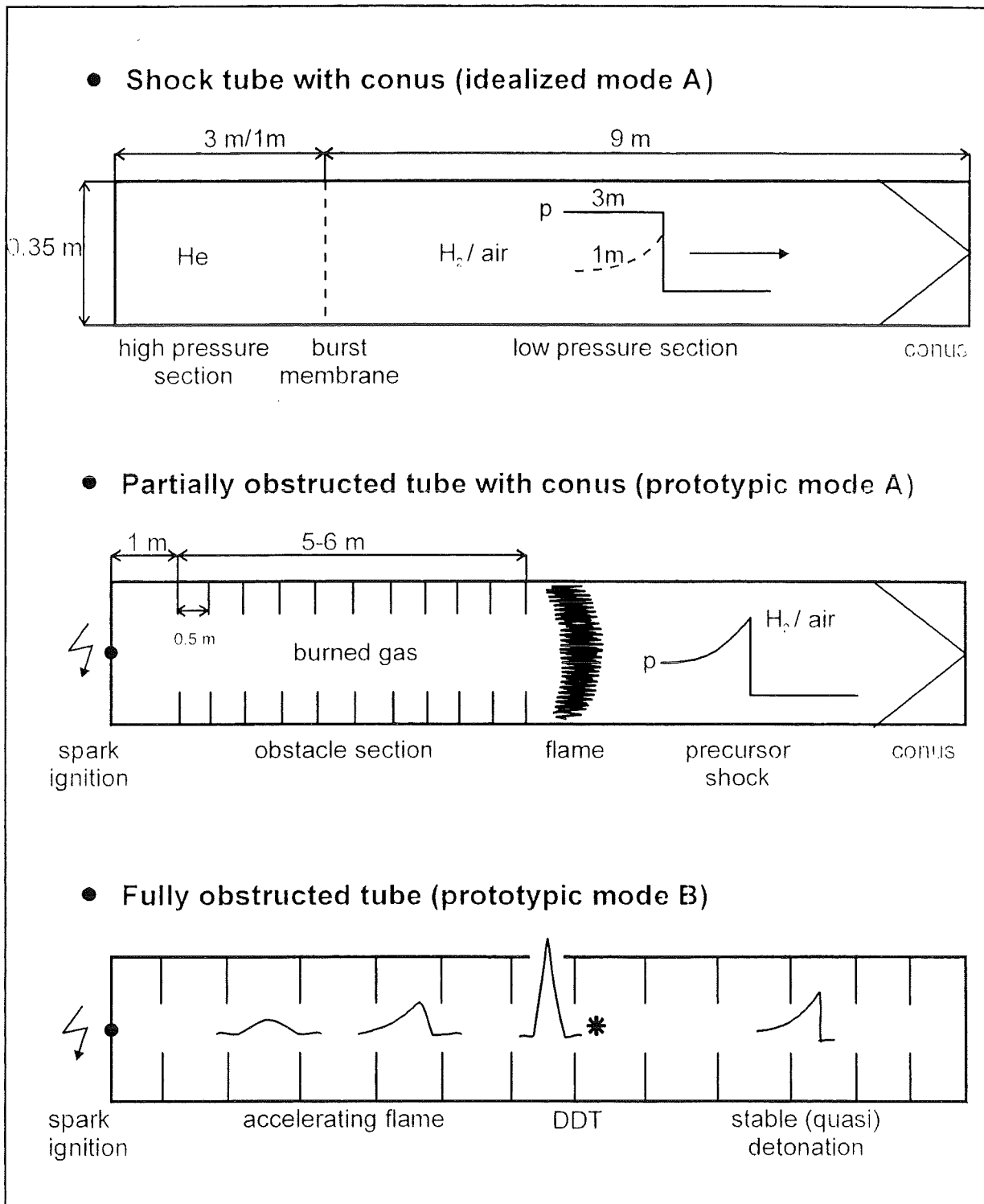


Fig. 2: FZK 12m tube and typical internal flow obstacles used for flame acceleration



**Fig. 3:** FZK experiments on DDT mechanisms using three experimental configurations of the 12 m tube. Instrumentation concentrated at expected DDT locations. Pressure transducers, photodiodes, film thermocouples, and ionisation gauges were installed.

## 2.2 Results of idealised mode A-DDT experiments

The experiments were carried out with a conus at the end of the low pressure section to focus the incoming pressure wave and to create conditions for self-ignition. The conus is used to produce local hot spots in the combustible gas as they develop in general from the interaction of a pressure wave with a complex multidimensional target. With the rotationally symmetric conus at the end of the tube the incoming shock wave is focused into a certain volume in the center of the conus, as depicted schematically in Figure 4.

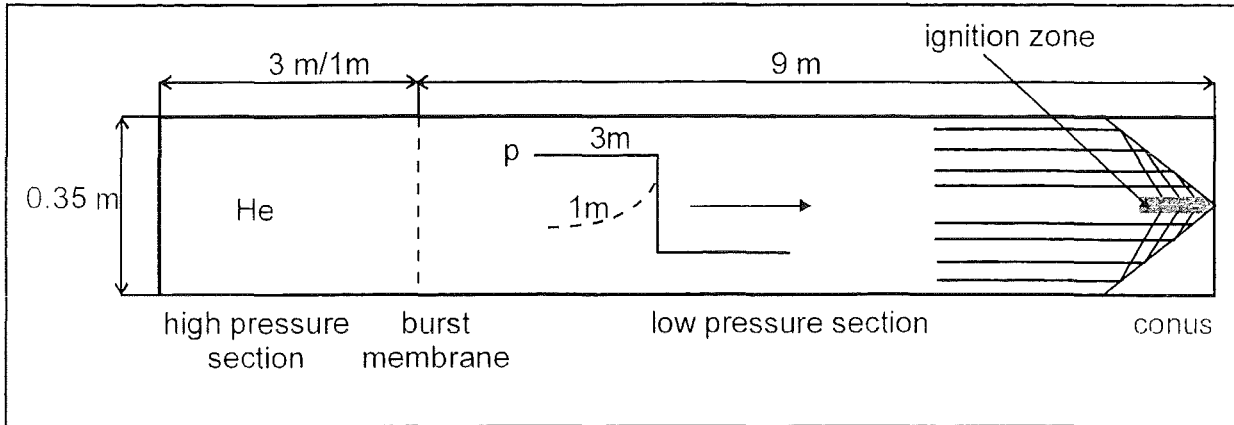


**Fig.4:** Focusing of the incoming shock wave in the center of the conus

Photographs and a scheme of the used conus are shown in Figures 4 and 5. The conus is 210 mm long with an opening angle of 70°.

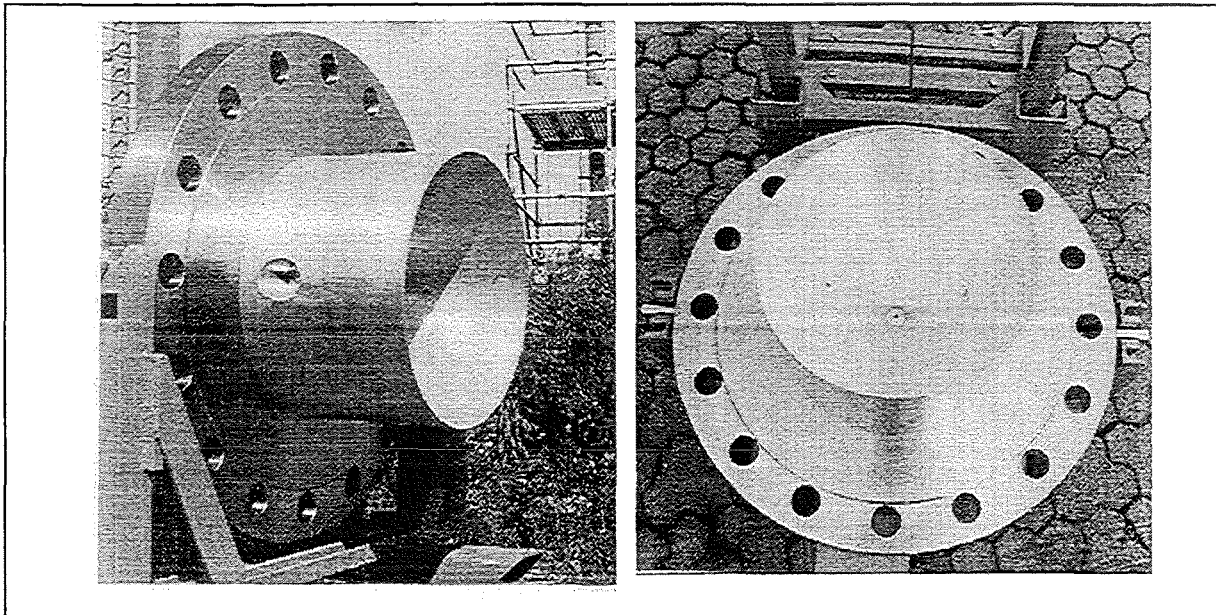


**Fig.5:** Photographs of the conus used to produce local hot spots for selfignition of the test gas. Three pressure transducers are installed inside the conus.

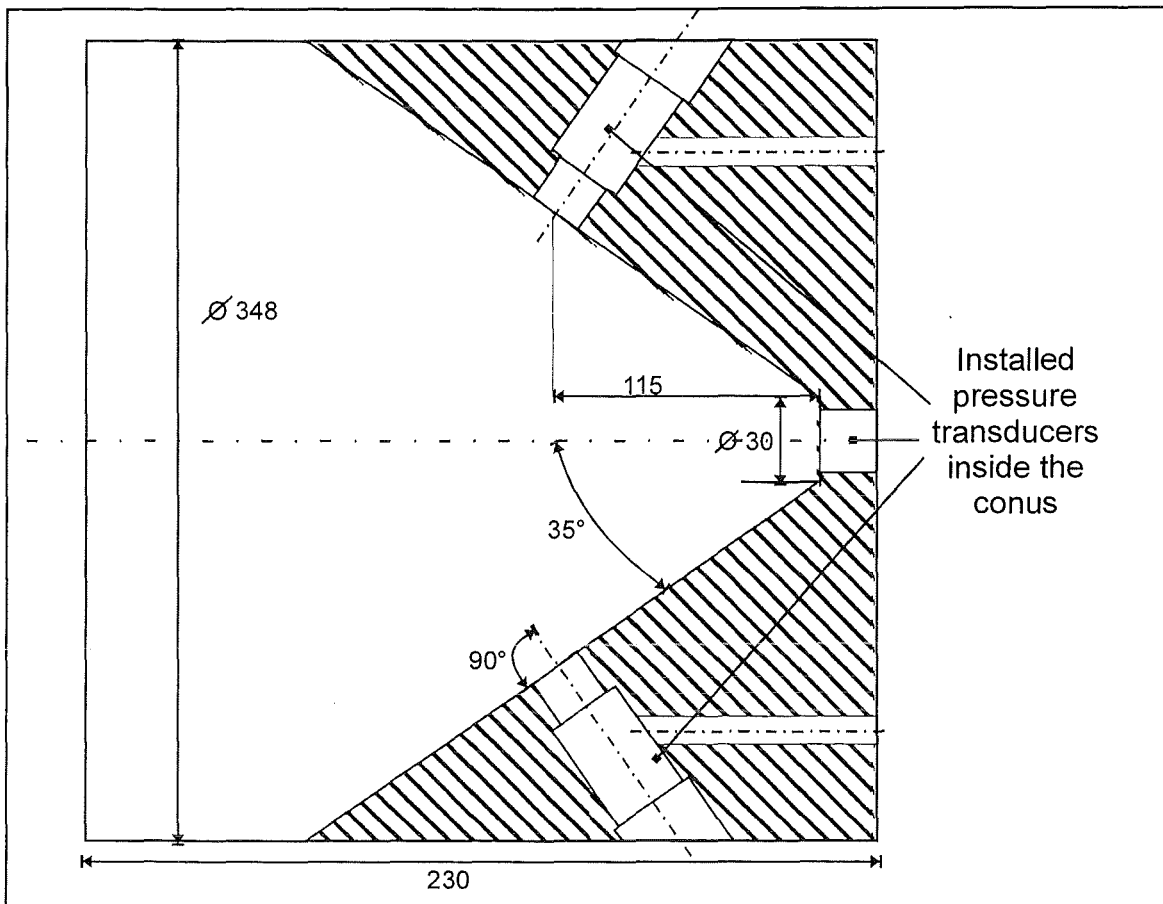


**Fig.6.:** Scheme of used conus with pressure transducer locations.

A total of 84 experiments were performed with the idealised-mode-A tube configuration. They are listed in Table 1, where  $p_0$  and  $p_4$  designate the initial pressure of the low and high pressure section, respectively. These experiments were carried out with helium as driver gas in the high pressure section (HPS). Aluminium foils with different thicknesses (0.1-0.7mm) were used as membranes. A further parameter was the length of the high pressure section which could be changed from 3m to 1m with an unchanged length of the low pressure section (9 m).

**Table 1:** Test matrix of DDT experiments in idealised mode A tube configuration

Experiment	Length of HPS (m)	%H <sub>2</sub>	$p_0$ (bar) LPS	$p_4$ (bar) HPS	Ma-number of incident wave	Velocity of reflected wave (m/s)
R0797_15	3	0	0.3	7	2.55	475
R0797_16	3	30	0.9	14	---	---
R0797_17	3	15	0.45	7.7	2.49	1006
R0797_18	3	30	0.9	7.8	---	---
R0797_19	3	15	1	8	1.99	1087
R0797_20	3	15	1.25	8.2	1.76	438
R0797_21	3	15	1.1	8.4	1.96	1128

Experiment	Length of HPS (m)	%H <sub>2</sub>	p <sub>0</sub> (bar) LPS	p <sub>4</sub> (bar) HPS	Ma-number of incident wave	Velocity of reflected wave (m/s)
R0797_22	3	0	1	8	1.94	414
R0797_23	3	15	1.2	8	2.13	1103
R0797_24	3	15	0.7	7.9	2.14	1086
R0797_25	3	15	1	7.2	---	---
R0797_26	3	15	0.8	5.15	---	---
R0797_27	3	13	1.1	7.9	1.84	430
R0797_28	3	13	1.25	6.8	1.66	436
R0797_29	3	17	1.25	8	1.7-1.72	443
R0797_30	3	13	0.7	7.4	---	---
R0797_31	3	17	1.1	6.9	---	---
R0797_32	3	14	1.1	6.75	---	---
R0797_33	3	14	0.8	6.25	1.902	490
R0797_34	3	12	1.1	6.0	1.72	431
R0797_35	3	12	0.8	6.2	1.8972	430
R0797_36	3	11	1.1	7.4	1.834	441
R0797_37	3	11	0.8	8.5	1.99	441
R0797_38	3	10	0.8	8.4	no measurement	---
R0797_39	3	10	1.1	8	1.815	430
R0797_40	3	9	1.1	8.3	1.839	426
R0797_41	3	9	0.8	7.8	1.94	423
R0598_00	3	15	1	8.3	1.875	410
R0598_01	3	15	0.950	8.95	1.93	500
R0598_02	3	15	0.9	8.3	1.925	1153
R0598_03	3	12	0.5	7.7	2.28	1041
R0598_04	3	11	0.4	7.6	2.37	949
R0598_05	3	12	0.6	6.1	2.0	961
R0598_06	3	12	0.7	7.7	2.11	1042
R0598_07	3	12	0.8	7.8	1.94	520
R0598_08	3	11	0.5	6.6	2.21	541
R0598_09	3	0	0.5	8.0	2.26	426
R0598_10	3	0	0.75	8.2	2.09	416

Experiment	Length of HPS (m)	%H <sub>2</sub>	p <sub>0</sub> (bar) LPS	p <sub>4</sub> (bar) HPS	Ma-number of incident wave	Velocity of reflected wave (m/s)
R0598_12	3	15	0.97	7.9	1.87	---
R0598_13	3	15	0.970	8.3	2.22	1171
R0598_14	3	11	0.450	7.0	2.265	893
R0598_15	3	12	0.750	7.2	2.09	500
R0598_16	3	12	0.72	7.6	2.15	1007
R0598_17	3	11	0.470	7.4	2.48	1056
R0598_18	3	15	0.970	7.4	2.01	1333
R0598_19	3	15	0.97	5.7	1.78	1293
R0598_20	3	15	1.15		1.8	1293
R0598_21	3	15	1	3	1.29	---
R0598_22	3	15	1	0.3	1.96	---
R0598_23	3	11	0.55	5.2	1.98	431
R0598_24	3	11	0.5	5.5	2.19	514
R0598_25	1	15	0.5	6.0	2.04	1172
R0598_26	1	15	0.7	6.5	1.77	480
R0598_27	1	0	0.7	6.0	---	---
R0598_28	1	0	0.5	6.3	1.86	442
R0598_29	1	15	0.6	6.0	1.73	474
R0598_30	1	15	0.5	7.0	1.93	506
R0598_31	1	15	0.45	7.0	2.03	1339
R0598_32	1	15	0.4	6.0	1.96	1230
R0598_33	1	15	0.4	6.0	1.996	1250
R0598_34	1	15	0.4	6.4	2.26	1119
R0598_35	1	0	0.4	7.3	2.09	466
R0598_36	1	12	0.4	9.4	2.35	1013
R0598_37	1	12	0.5	8.2	2.05	487
R0598_38	1	12	0.4	9.5	2.27	1041
R0598_39	1	12	0.45	9.9	2.18	1071
R0598_40	1	12	0.5	9.0	2.09	500
R0598_41	1	0	0.6	11	2.05	457

R0598_42	1	0	0.45	12.5	2.26	468
R0598_43	1	11	0.4		2.64	1071
R0598_44	1	11	0.45	11.0	2.45	1056
R0598_45	1	11	0.5	12.0	2.19	514
R0598_46	1	11	0.48	11.8	2.31	1027
R0598_47	1	11	0.49	11.7	---	---
R0598_48	1	10	0.3	6.0		
R0598_49	1	10	0.35	---	---	---
R0598_50	1	10	0.35	7.2		
R0598_51	1	15	1.15	6.0		
R0598_52	1	15	0.93	6.6		
R0598_53	1	15	0.95	6.0		
R0698_00	1	10	---	---	2.07	490
R0698_01	1	10	0.4	12.95	2.8	1042
R0698_02	1	10	0.4	10.0	2.3	962
R0698_03	1	10	0.45	10.0	2.496	974
R0698_04	1	10	0.47	12.2	2.38	949
R0698_05	1	10	0.47	12.0	2.88	939
R0698_06	1	10	0.43	13.2	2.6	948
R0698_07	1	10	0.46	10.0	2.35	947

The different lengths of the HPS result in different flow fields. The principal processes in the shock-tube with a three meter long high pressure section are shown in the upper part of Figure 6. After membrane rupture, a shock wave propagates forwards from the membrane into the low pressure section. At the same time a rarefaction wave runs backwards into the high pressure section. The contact surface, which separates the driver gas of the high pressure section from the flammable mixture in the low pressure section, moves behind the incident shock into the low pressure section. The incident shock wave is reflected at the end of the low pressure section, it interacts with the contact surface and slows it down. The rarefaction wave propagates into the high pressure section and is reflected at the end of the tube. In this case, the reflected rarefaction wave meets the contact surface later than the reflected shock wave. The flammable mixture is located only between the contact surface and the end of the low pressure section. Only this part is available for ignition.

The lower diagram in Figure 7 shows the same process with a shortened high pressure section of 1 m. The processes after bursting of the membrane are the same as with the 3m high pressure section, but the rarefaction wave in the high pressure section is reflected earlier. It arrives at the contact surface before this hits the

reflected incident shock wave. The interaction between the reflected rarefaction wave and the contact surface leads to a velocity decrease of the contact surface. The lower diagram in Figure 7 shows, that the distance between the contact surface and the end of the low pressure section in this case is larger than in the first diagram. Therefore an extended space and time region exists in which the transition from deflagration to detonation could occur. The second effect of the shortened HPS is that the shape of the incident shock wave changes from a flat pressure profile to a triangular profile, which is typical for blast waves. Using the short HPS allowed therefore to investigate the effect of a changed pressure profile (shock wave versus blast wave).

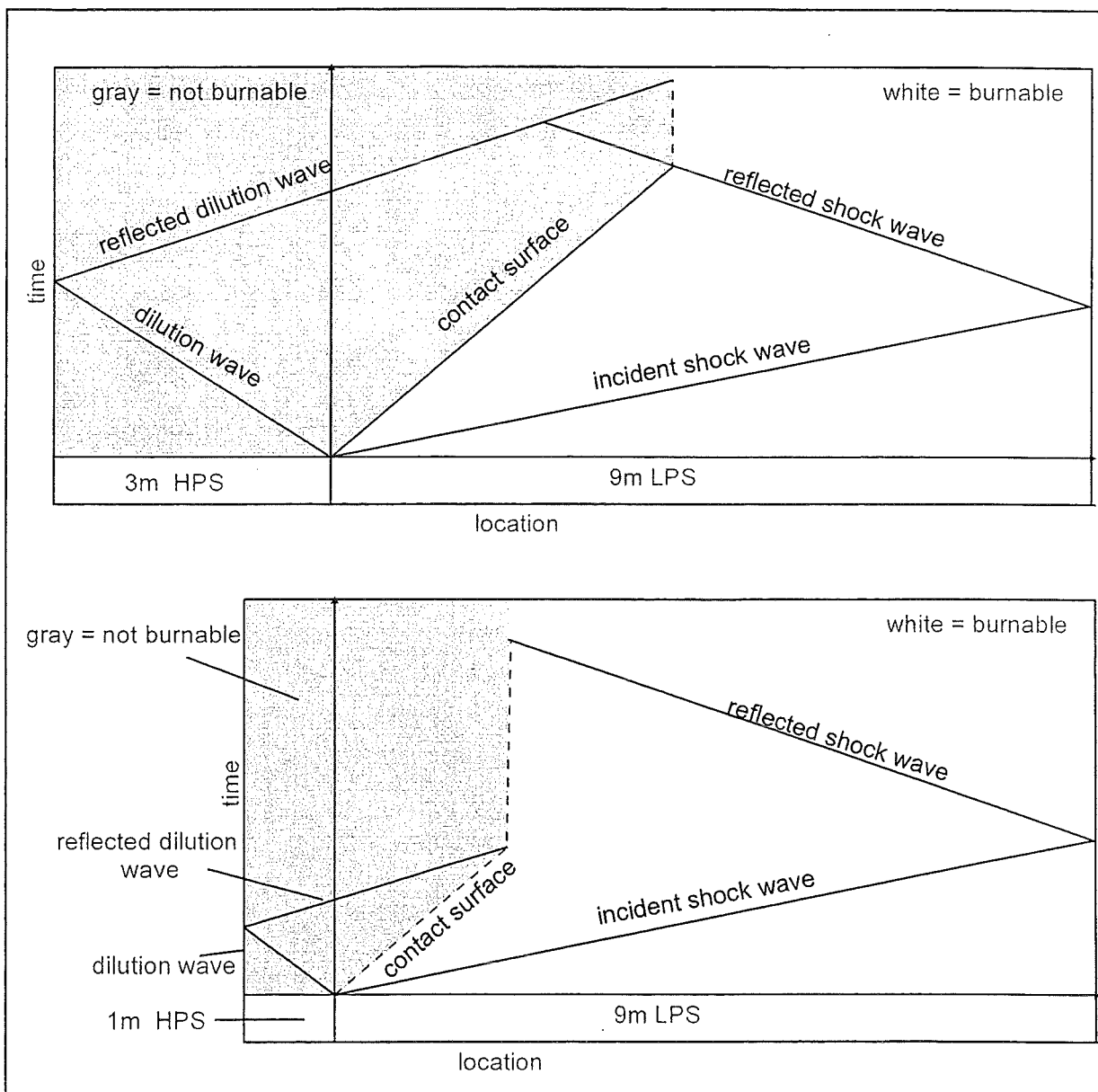


**Fig.7:** Principle processes in the shock tube with a 3 m and 1 m long high pressure section, respectively.

The main results of the idealised-mode-A tests are presented now by two examples: one for a mild ignition case without DDT, and one for a strong ignition leading to DDT. In both cases the short HPS with 1 m length was used. Figure 8 summarises the results of experiment R0598\_26 in the form of an R-t diagram. It shows the incident shock wave (ISW), the reflected shock wave (RSW) and the flame front (FF). The ISW and the RSW were measured with pressure transducers, the FF was detected with photodiodes. The test parameters used in this experiment were 15 % hydrogen in air with an initial pressure in the low pressure section of 0.7 bar. The high pressure section was filled with helium up to the burst pressure of 6.5 bar, resulting in a Mach number of 1.77. The test led to self-ignition and a decoupled flame / shock complex without DDT, which can be concluded from the fact that the ISW ignites the mixture, but the RSW moves faster than the FF. For the resulting RSW a velocity of 480 m/s was measured. This velocity is comparable to that of a normally reflected inert shock wave without reaction, again indicating that only a weak combustion pressure was generated by the ignition.

An example for selfignition and formation of a coupled flame / shock complex, leading to a stable detonation wave (DDT) is shown in Figure 9. This R-t diagram was recorded during experiment R0598\_25. The test parameters used in this experiment were 15 % hydrogen in air with an initial pressure of 0.5 bar. The high pressure section was filled with helium up to a burst pressure of 6.0 bar, resulting in a Mach number of 2.04. The triangular shape of the incident shock wave is clearly visible. Again the ISW is focused in the conus thereby igniting the mixture, but this time the resulting RSW and the FF remain coupled. The measured velocity of the RSW is 1172 m/s, which is close to the theoretical detonation speed in the moving H<sub>2</sub>/air mixture. (The wave speed  $w$  in the laboratory frame is  $D$  minus the particle velocity  $u_2$  behind the incident shock,  $w=D-u_2$ )

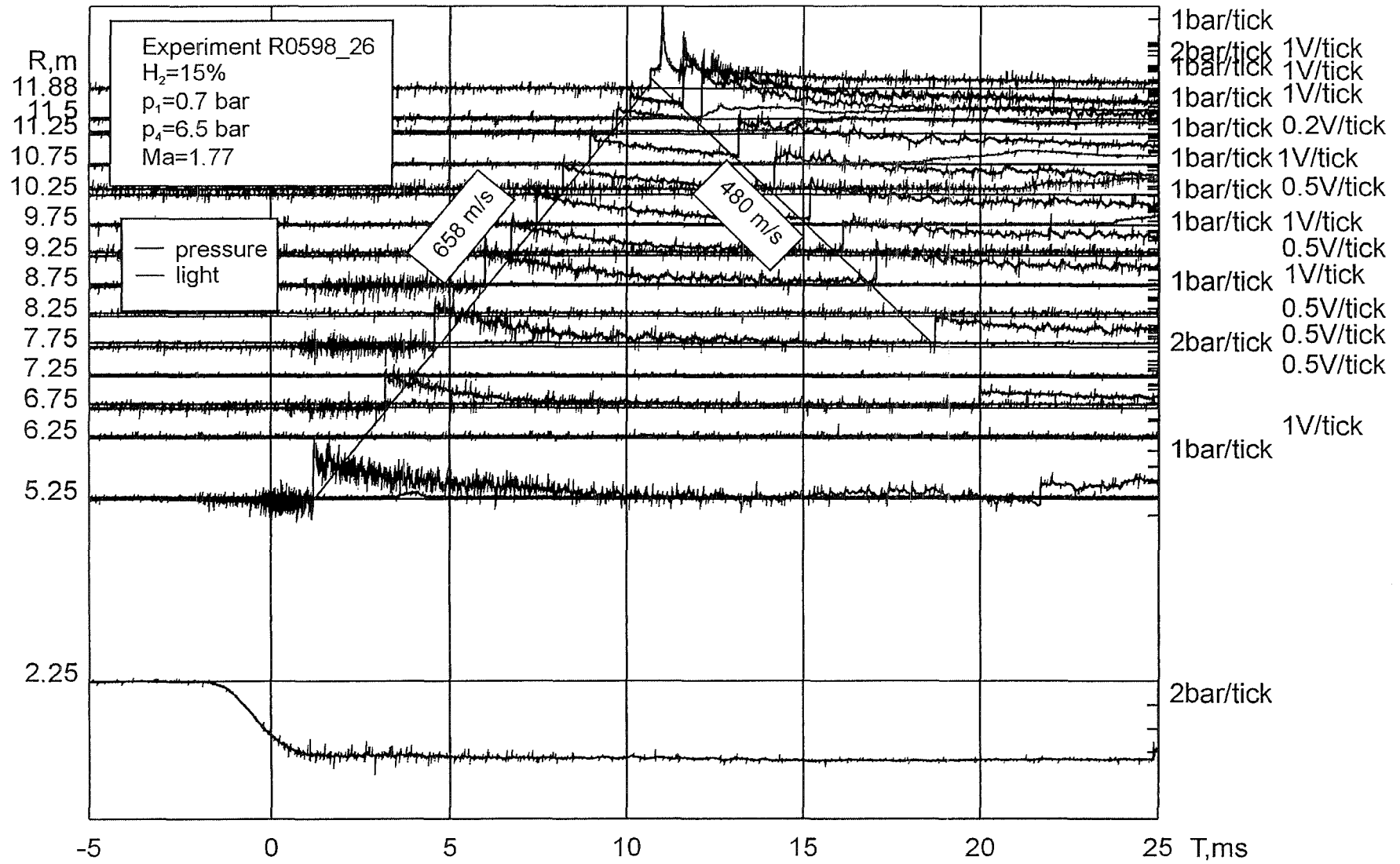


Fig.8: Measured light and pressure signals for experiment R0598\_26. Example for mild ignition without DDT.

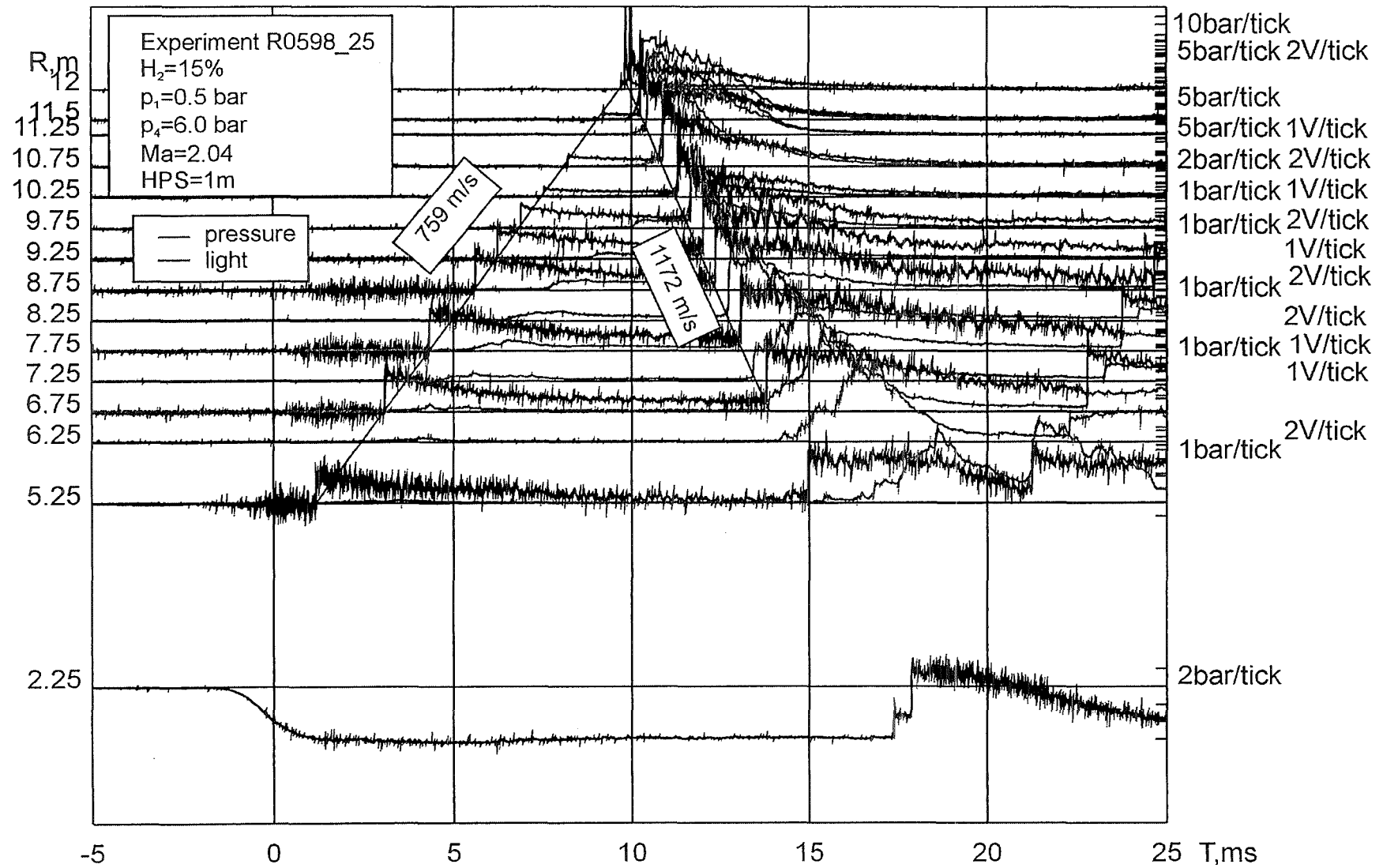
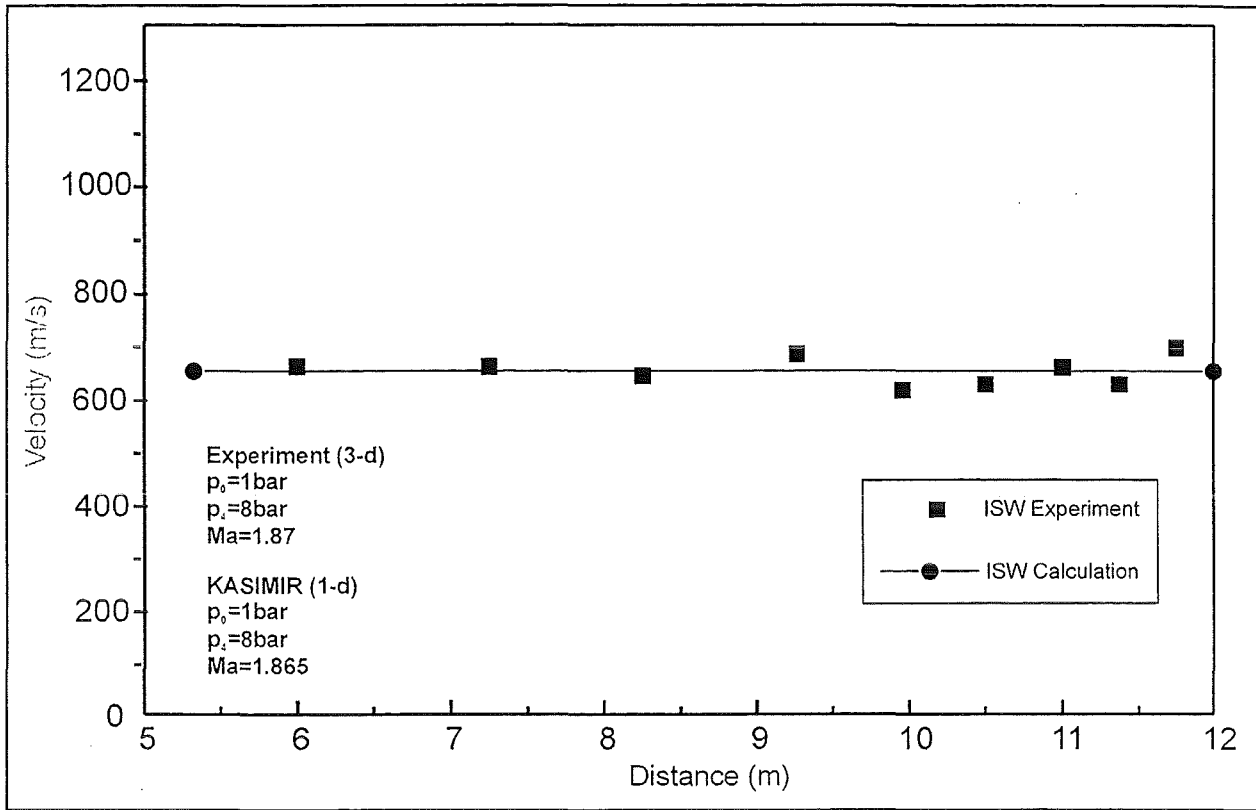


Fig.9: Measured light and pressure signals for experiment R0598\_25. Example for strong ignition with DDT.

To verify if the shock wave velocities measured in the experiments correspond to theoretical shock wave velocities, calculations with the KASIMIR code were performed.



**Fig.10:** Comparison between KASIMIR calculation and FZK tube experiment.

KASIMIR is a one-dimensional program which was developed at the Shock Wave Laboratory of RWTH Aachen to describe the dynamics of waves in shock tubes. Figure 10 shows a comparison between the calculated velocity of the incident shock wave with KASIMIR and the velocity of the shock wave in the experiment under equal conditions. Although the experiments are of three-dimensional nature the average shock wave velocity agrees well with 1-d KASIMIR calculations. Contrary to the calculation, the membrane fails in the experiment not as a flat surface, but rather as a hemispherical surface, which creates additional transverse waves in the tube.

Based on the R-t diagrams of the experiments t-x diagrams were constructed for the different observed wave trajectories. Figures 11, 12 and 13 show examples for experiments with different hydrogen concentrations and Mach numbers of the ISW.

Figure 11 shows the t-x diagrams for two experiments with 11 % hydrogen. The upper experiment resulted in a Mach number of 2.19 for the incident shock wave. The ISW travels with a velocity of 870 m/s through the shock tube, is focused in the conus and thereby ignites the mixture. The measured velocity of the RSW is 514 m/s. This velocity is comparable to that of a normally reflected inert shock wave without reaction. The RSW and the FF decouple very early, about 1m away from the conus. The lower test gave a Mach number of 2.48 for the incident shock wave (900 m/s). The velocity of the RSW was measured to 1056 m/s which is close to the theoretical detonation speed in the moving gas. The RSW and the FF remain

coupled over a distance of 4.5 m from the conus. A separation of the flame / shock complex appears only after arriving near the contact surface (He/H<sub>2</sub>-air interface) where the combustion is necessarily quenched.

Figure 12 also shows the t-x diagrams for two experiments with 12 % hydrogen in air and different Mach numbers of the ISW. The experiment with the lower Mach number again leads to a velocity of the RSW (500 m/s) which is comparable to an inert RSW. Again the RSW and the FF decoupled close to the conus ( $\leq 1\text{m}$ ). The experiment with the higher Mach number leads to a velocity of the RSW (1041 m/s) which is close to the theoretical detonation speed. In this case FF and RSW decouple about 4m away from the conus.

The t-x diagrams for two experiments with 15% hydrogen in air and different Mach numbers of the ISW are shown in Figure 13. Similar to Figures 10 and 11 the lower Mach number (1.93) of the ISW leads to a RSW with a velocity characteristic for inert behaviour (506 m/s), where as the higher Mach number of the ISW (2.01) leads to a typical detonation velocity of the RSW (1333m/s). Also in this case the decoupling of RSW and FF is earlier in the experiment with lower ISW Mach number of (2m after conus) than in the experiment with higher Mach number (4m after conus).

To check whether the detonation mode of the experiment is stable or unstable the position of the contact surface was calculated with the one-dimensional KASIMIR program (shown in Figures 11, 12 and 13). In the experiment with 11 % H<sub>2</sub> and an ISW Mach number of 2.48, the detonation seems to be stable because the RSW and FF decoupled only after arrival of the contact surface. In the experiment with 12% hydrogen in air ( Mach number of 2.28 ) and in the experiment with 15 % hydrogen in air ( Mach number 2.01 ), the RSW and the FF decouple somewhat before the calculated arrival of the contact surface. Therefore in these cases the detonation may not to be fully stable, or may transit into a galloping regime.

Three criteria can be used to determine whether DDT occurred or not. The first is the velocity of the reflected wave, the next coupling or decoupling of pressure and light signals, and a further method is to analyse the pressure amplitudes and profiles along the tube. Therefore at given times the pressures at each pressure transducer location were collected and depicted as function of tube location. This was done for different times in each experiment. The spatial distribution of the pressure gives clear indications about the existence of DDT-processes.

An example for pressure profiles along the tube without ignition and combustion (inert case) is given in Figure 14. The upper part shows the measured pressure

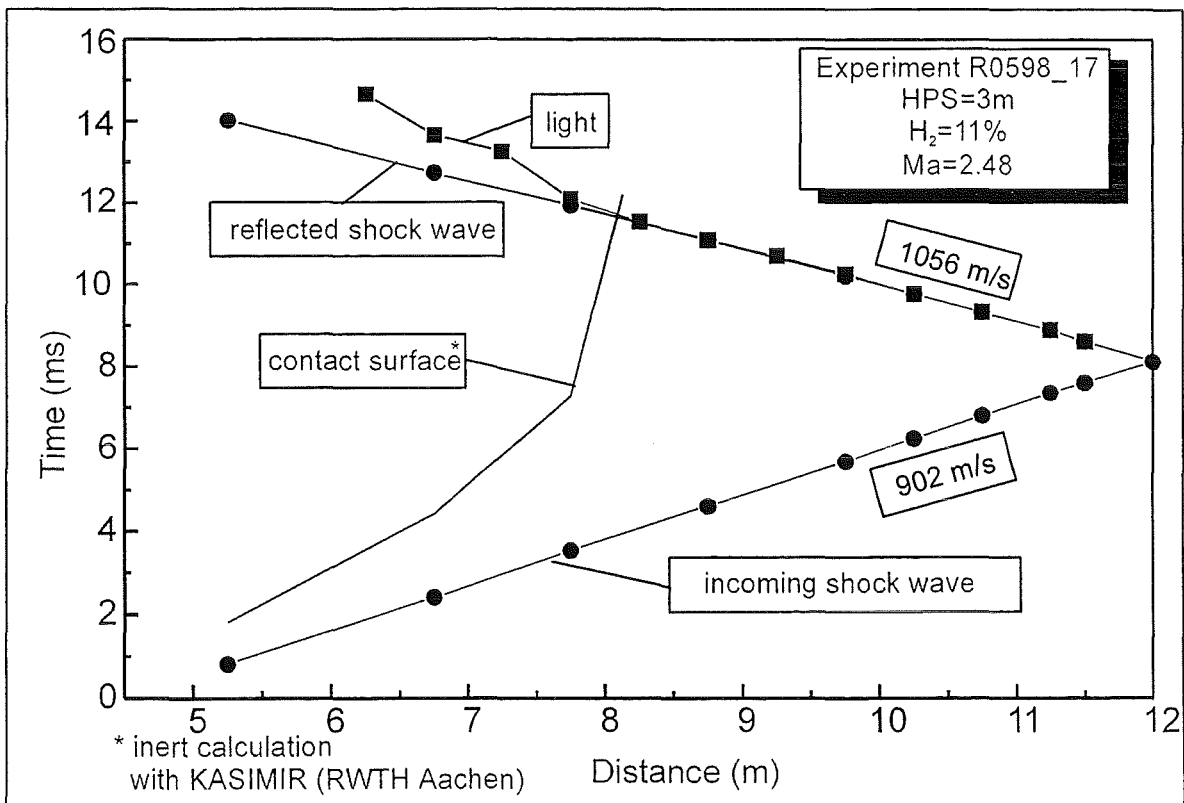
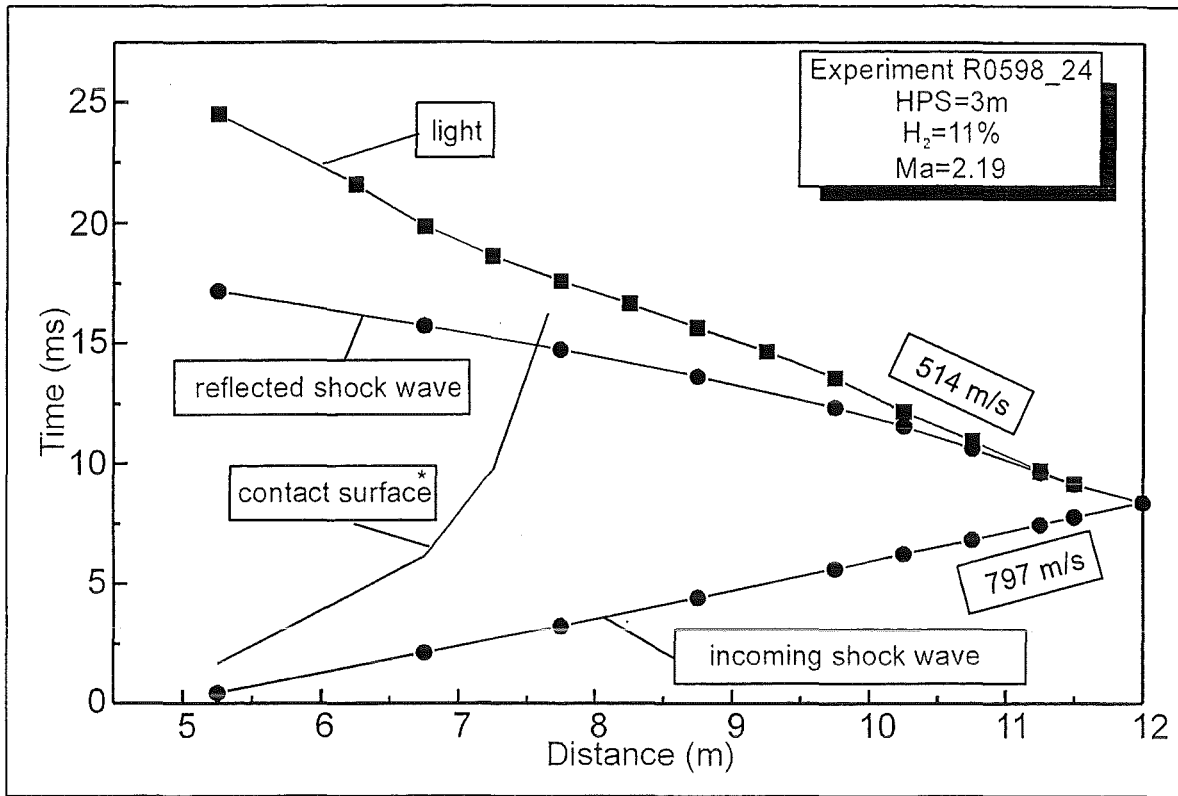
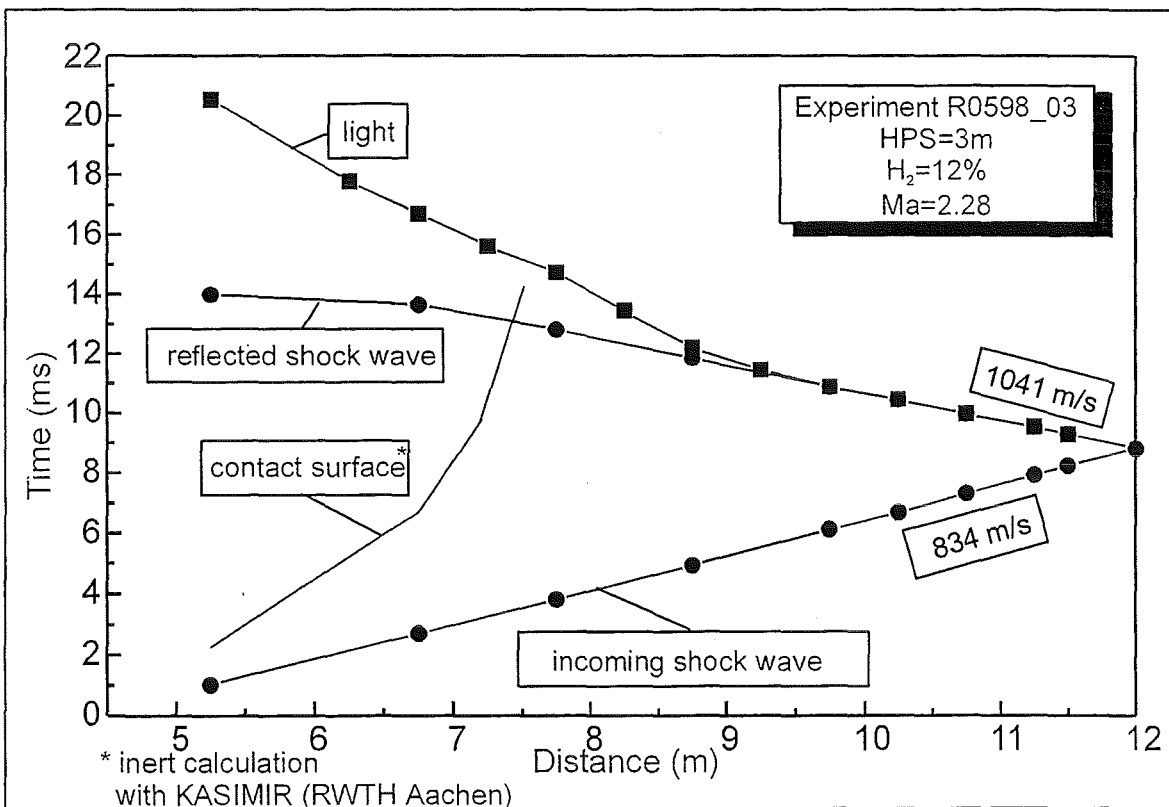
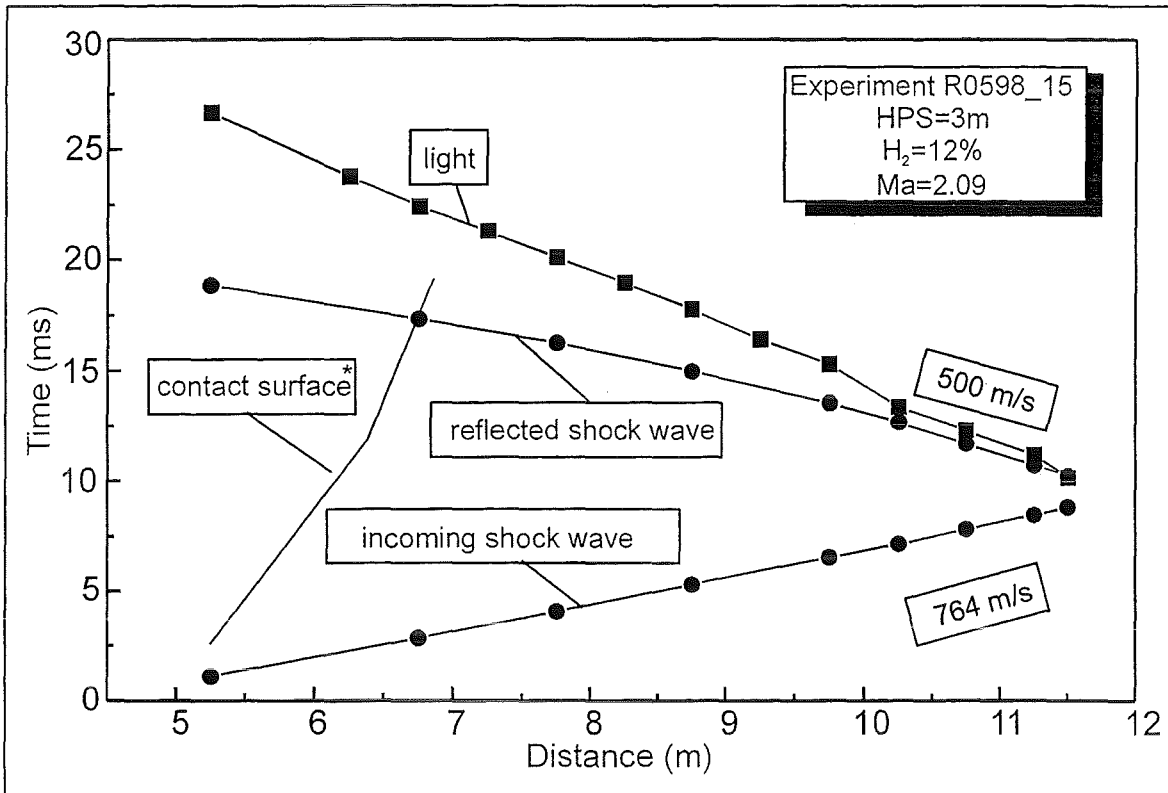


Fig.11: Example for measured light and pressure trajectories with for 11% hydrogen. Upper case weak ignition without DDT, lower case strong ignition with DDT.



**Fig.12:** Example for measured light and pressure signals with 12% hydrogen. Upper case weak ignition with uncoupling of pressure and flame front (no DDT), lower case strong ignition with coupling (DDT).

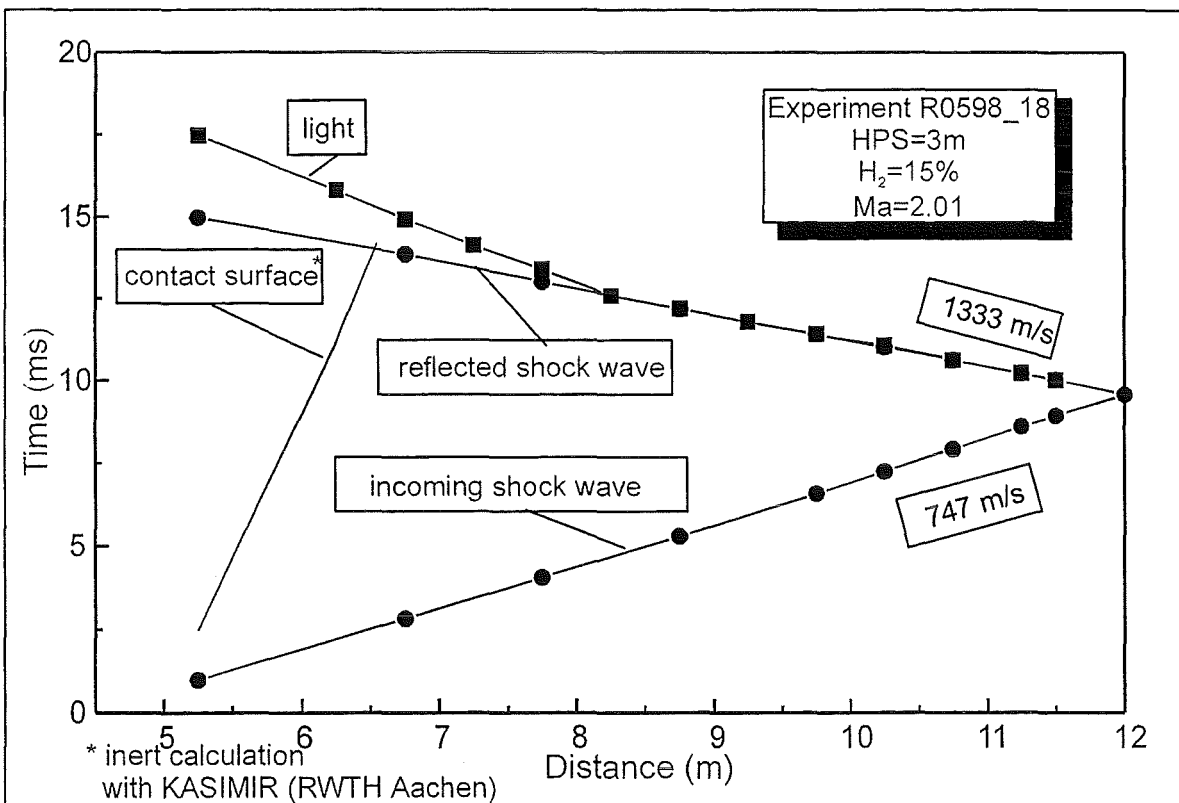
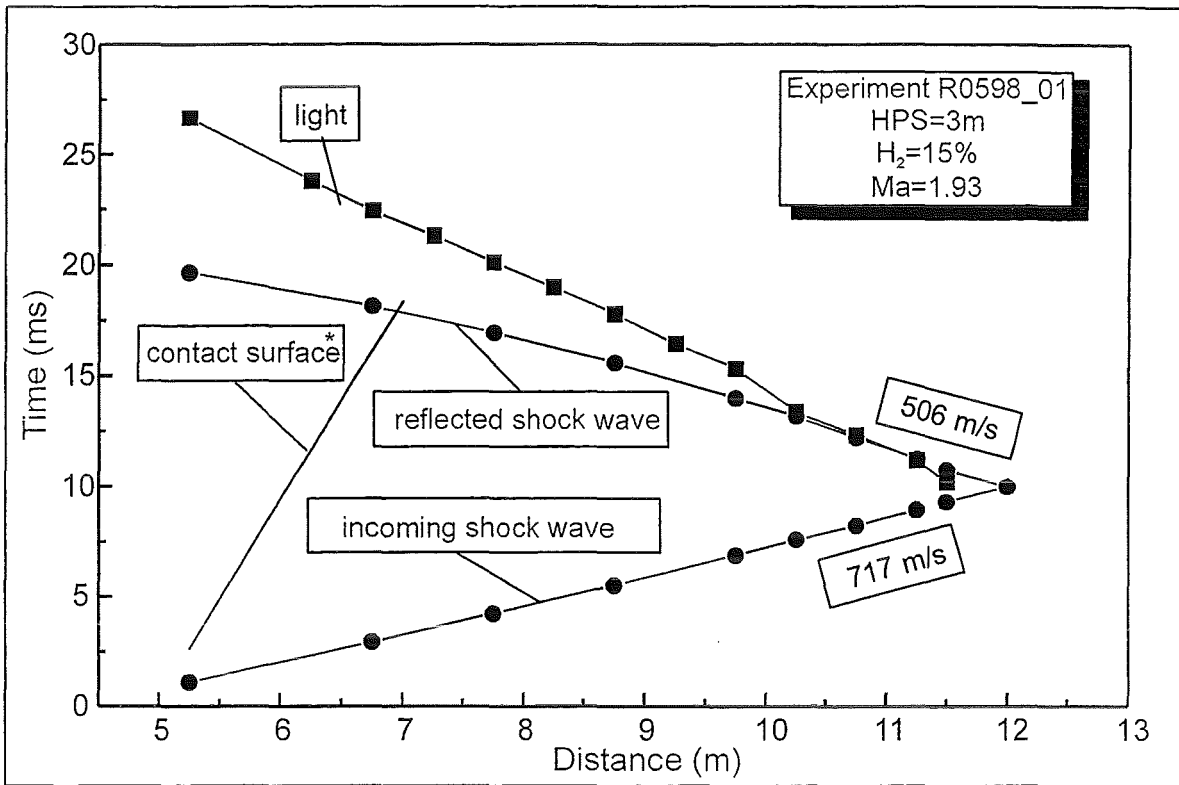
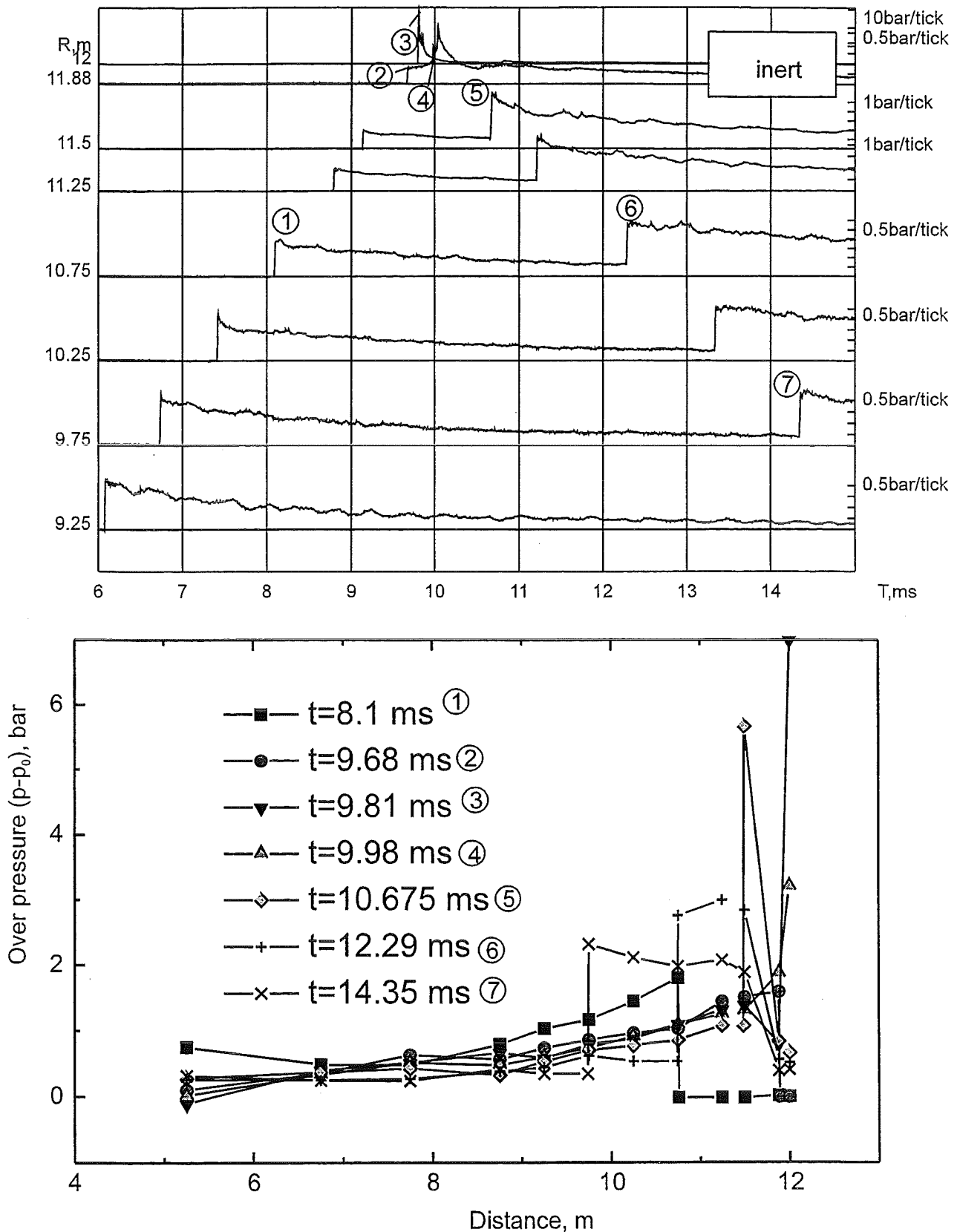


Fig. 13: Example for measured light and pressure signals for 15% hydrogen. Upper case with weak ignition (uncoupling of pressure and flame front), lower case with strong ignition and DDT (pressure/flame complex, detonation typical speed or RSW).

histories of experiment R0598\_35 with the following initial conditions: 0 % hydrogen,  $p_0=0.7$  bar,  $p_4=7.3$  bar. The short HPS section was used. The measured Mach number of the ISW was 2.09 and the reflected wave speed was 466 m/s. The times at which the pressures along the tube were evaluated from the R-t diagram correspond to the arrival times 1 to 7 of the shock at the transducer locations.

Curves 1 and 2 in the lower part of Fig.14 show the typical incoming shock front pressures in an inert case. Curves 3-7 in the lower part of Fig.14 show typical reflected shock pressure distributions for an inert case. The maximum pressure which is created by focusing in the conus decays rather fast with increasing distance from the conus. Although the shown pressures scatter somewhat from the noise in the  $p(t)$  data, they show typical reflected pressure profiles for the case of an inert mixture. The low pressures of reflected waves inside the conus are due to the change of cross section area in this reflector.



**Fig.14:** Measured pressure histories of experiment R0598\_35 (top) and pressure profiles along the tube at given times (bottom). Inert test without hydrogen. (Initial conditions: 0% hydrogen,  $p_0=0.7$  bar,  $p_4=7.3$ bar,  $Ma=2.09$ . Measured velocity of RWS=466 m/s).

An example for nearly the same initial conditions ( $p_0=0.7$ ,  $p_4=6.4$ ,  $Ma=1.77$ ,  $RSW=480$  m/s) but with 15 % hydrogen is given in Figure 15. The curves 1 and 2 in the lower part of Fig.15 show pressure profiles of the incoming shock wave. Curves 3-6 show reflected pressure profiles, but in comparison to the experiment without hydrogen, the maximum measured pressure in the conus is much higher (8 bar inert case, 40 bar with hydrogen). Also the reflected pressures outside of the conus show higher values. These higher pressures are an effect of the deflagrative combustion process which started inside the conus.

The pressure histories of experiment R0598\_31(initial conditions:  $Ma = 2.03$ ,  $RWS = 1399$  m/s) which is given in Figure 16 shows a rather different behaviour in comparison to the inert experiment (R0598\_35) and the experiment with mild ignition R0598\_26. The pressure profiles of the incoming shock show of course the same behaviour as in an the inert case, but the shape of the reflected pressures resembles closely that of CJ-detonations. Note that the initial pressure in the LPS was only 0.45 bar which indicates that the detonation decays from an overdriven state towards CJ-conditions as it propagates away from the reflector. In addition the higher velocity and also the coupling between light and pressure leads to the conclusion that DDT occurred in this experiment.

Based on these three indicators ( reflected wave speed, coupling between light and pressure, magnitude and shape of pressure distribution ) the experiments could be grouped clearly into cases with and without DDT.

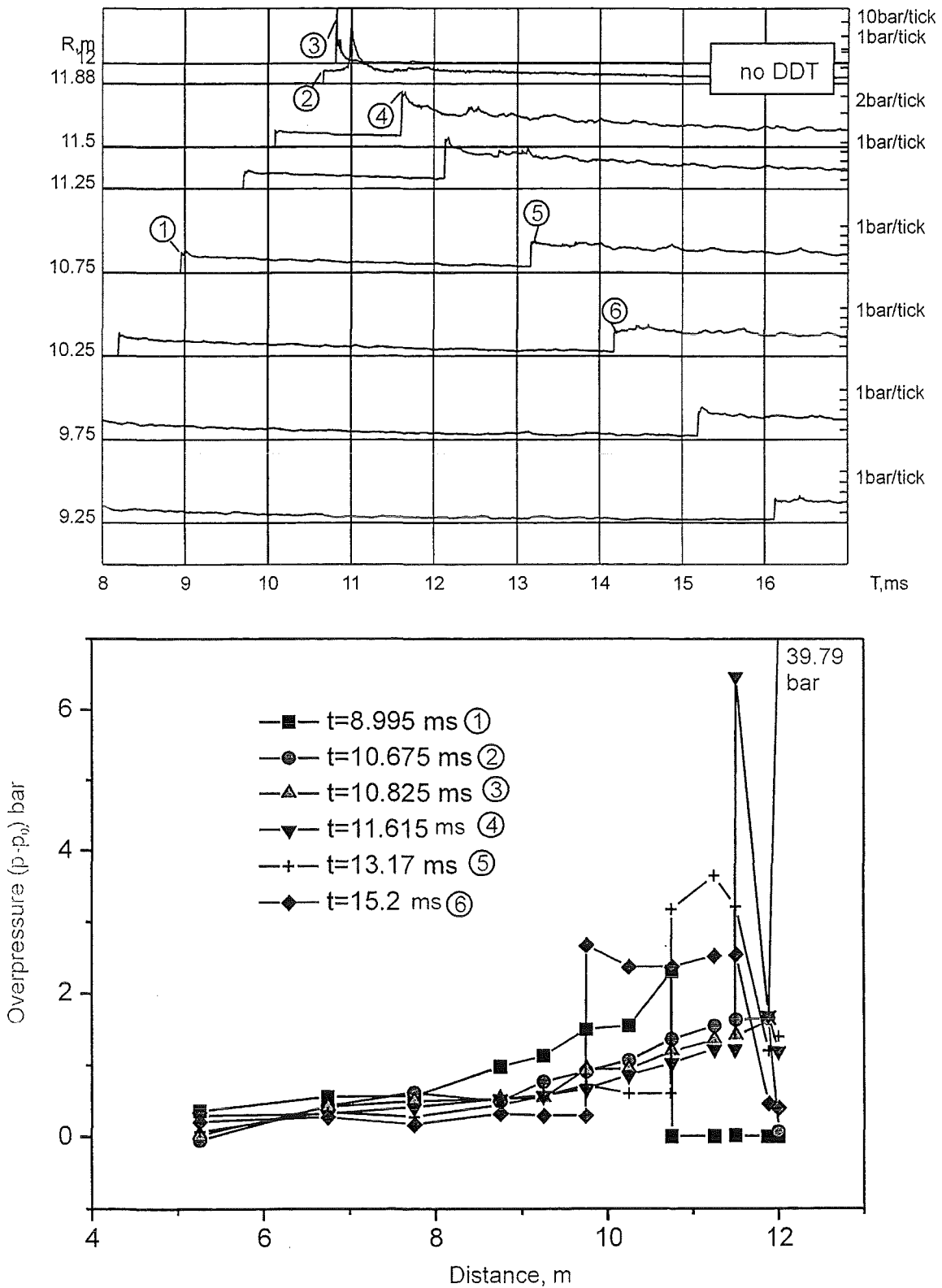
Figure 17 (3m high pressure section) and Figure 18 (1m high pressure section) summarise all FZK-experiments as function of the Mach number of the ISW and the hydrogen concentration in air. These data were obtained in joint FZK/RAS measurement campaigns. The experiments can be classified into two groups:

- The first (lower) area describes an uncoupled propagation of RSW and FF with time and length differences of  $dt = 1-2$  ms and  $dL=0.5-1$ m. Measured reflected pressure amplitudes and profiles along the tube are comparable to inert cases, indicating absence of DDT.
- The second (upper) area describes a regime of coupled propagation of RSW and FF with  $W + u_2 \approx D$ , which confirms DDT ( $W$ =measured wave speed in laboratory frame,  $u_2$  = particle velocity,  $D$ = CJ detonation speed in stationary gas). DDT is further supported by the pressure amplitudes and typical detonation pressure profiles along the tube.

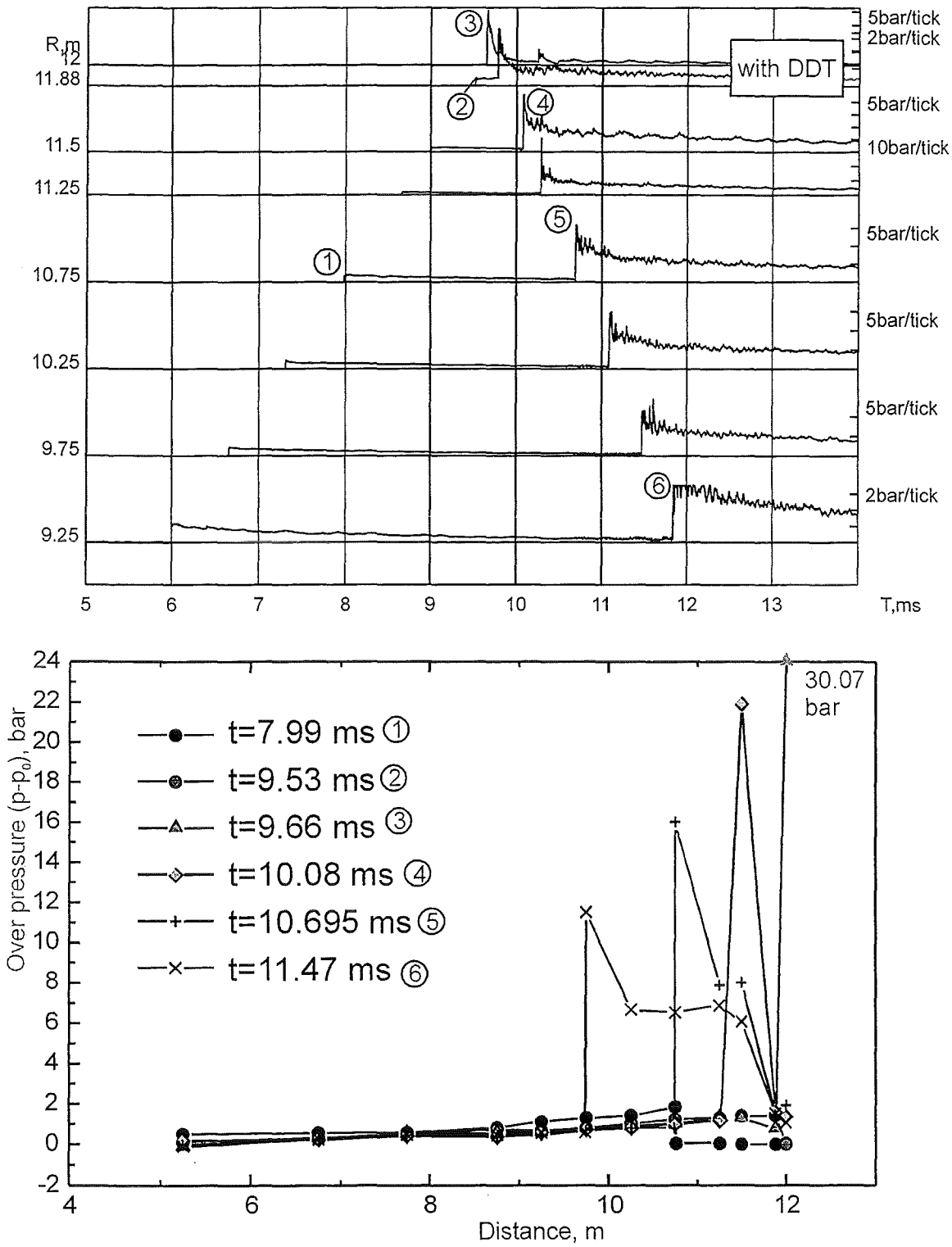
The small triangular region in Fig. 17 between no-DDT and DDT- conditions shows the remaining parameter space which was not covered by experiments. This narrow gap demonstrates that a well defined critical Mach number exists for a given hydrogen concentration in air above which DDT occurs.

Figure 18 summarises the experiments with a shorter HPS (1m) The shadowed area in the middle again depicts the range in which the critical Mach number can be anticipated. Additional experiments would be required to further narrow down the borderline between DDT and no DDT behaviour in the investigated geometry.

Figure 19 summarises the dependence of the RSW velocity on the Mach number of the ISW for 10%, 11 %, 12.% and 15 %  $H_2$  in air. For 10 % hydrogen in air the



**Fig: 15** Measured pressure histories of experiment R0598\_26 (top) and pressure profiles along the tube at given times (bottom). Initial conditions: 15% hydrogen,  $p_0=0.7$  bar,  $p_4=6.7$  bar,  $Ma=1.77$ . Measured velocity of RWS=480 m/s).



**Fig: 16** Measured pressure histories of experiment R0598\_31 (top) and pressure profiles along the tube at given times (bottom). (Initial conditions: 15% hydrogen,  $p_0=0.45$  bar,  $p_4=7.0$  bar,  $Ma=2.03$ ,  $RWS=1399$  m/s)

critical Mach number of the ISW is between 2.1 and 2.3, for 11 % hydrogen in air it is near 2.2, for 12 % hydrogen in air it is 2.1 and for 15 % hydrogen it is 1.93. We find that the critical Mach number of the IWS decreases with increasing hydrogen concentration, probably because smaller temperature increases are required for triggering a successful DDT.

Figure 19 demonstrates that no substantial difference could be observed between the experiments with 1 m and 3 m length of the HPS, respectively. Obviously the change in the pressure profile of the ISW obtained with the shorter high pressure section, causing a more triangular pulse with the 1 m length than with the 3 m length, did not substantially influence the overall DDT process. Recent numerical simulations [2] have indicated that the temperature gradients which are produced by the triangular incoming pressure pulse using a 1m long HPS (in HPS) are too small to create an additional SWACER mechanism, compared to the 3m HPS.

Figure 20 shows a summary plot containing the data points from Fig.19 and additional test results with more sensitive H<sub>2</sub>-air mixtures (22 and 30% H<sub>2</sub>). The dashed lines indicate the critical Mach numbers for the respective mixtures at which the reflected wave velocity suddenly switches from inert reflection values (lower line) to detonation like values (upper line). A very low Mach number was found for stoichiometric H<sub>2</sub>-air mixtures, demonstrating that DDT by mode A can be easily achieved if such mixtures should be present in a multidimensional enclosure and a pressure wave should be generated by a fast flame or by other means.

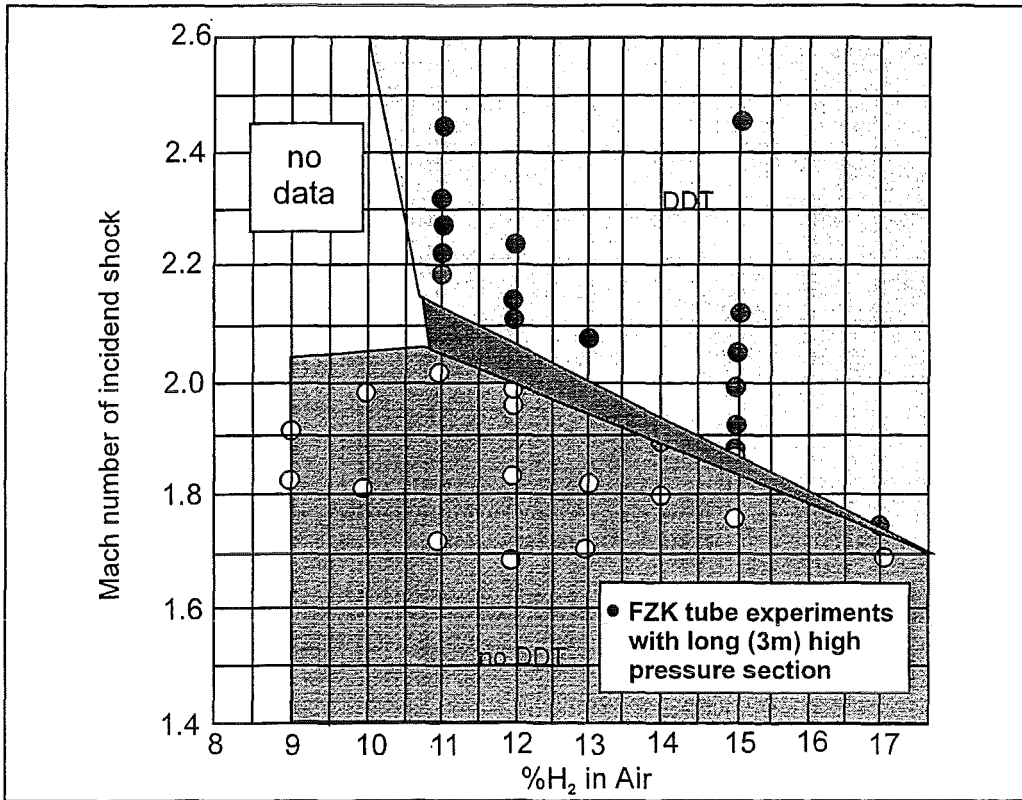


Fig 17: Critical Mach number for DDT in hydrogen -air mixtures (3m HPS)

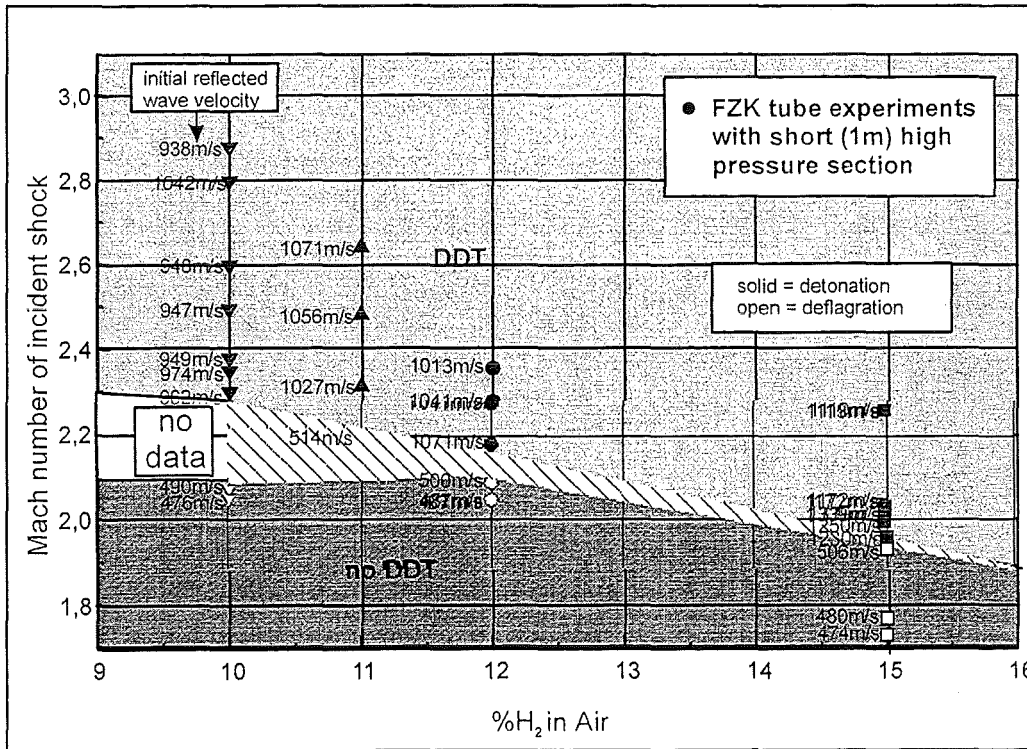
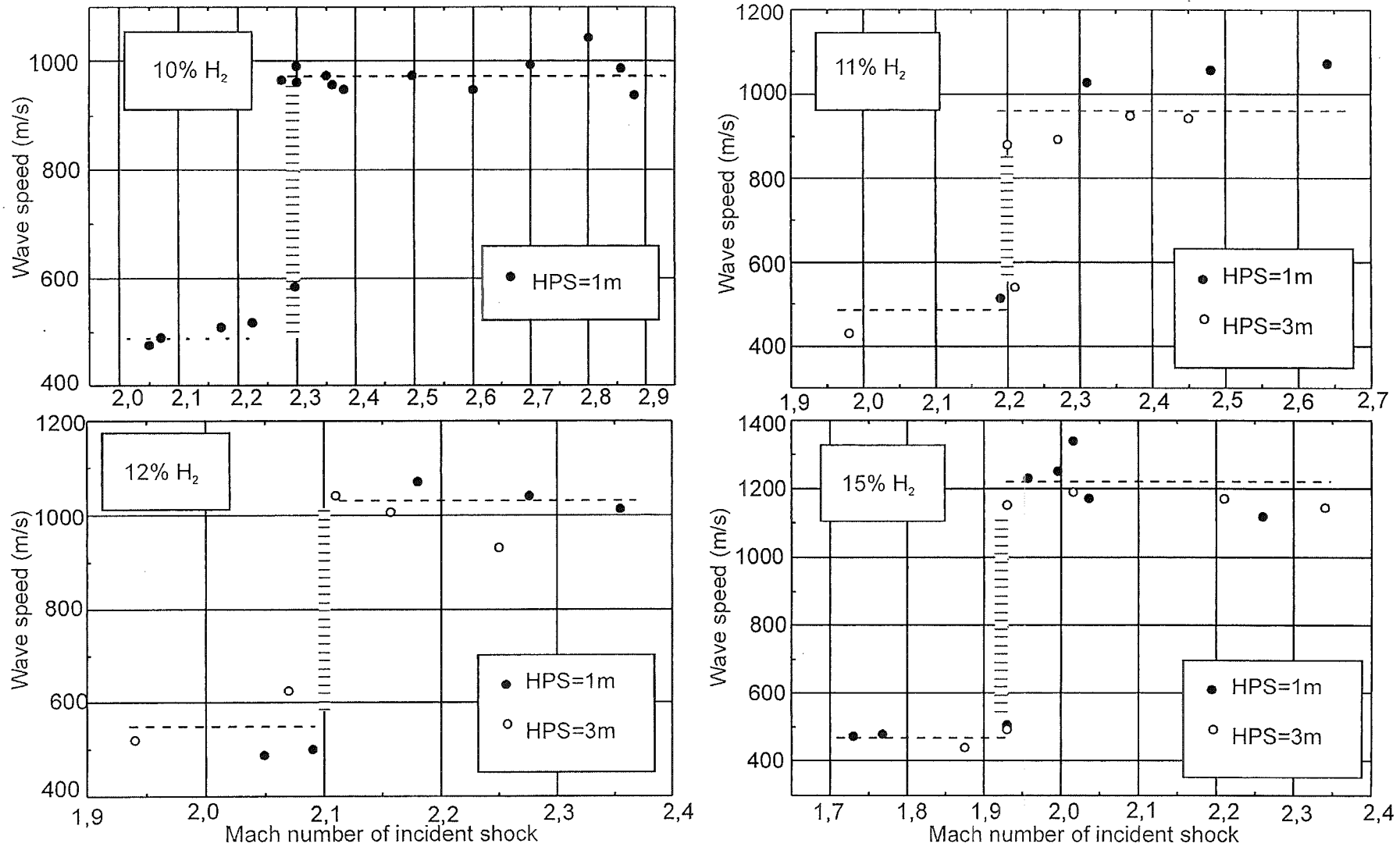


Fig.18: Critical Mach number for DDT in hydrogen -air mixtures (1m HPS). For each test the velocity of the reflected wave is included as indicator for deflagration (no DDT) or detonation (DDT).



**Fig.19:** Measured reflected wave speeds in idealised mode A-DDT-experiments. Tests with different pulse shapes (length of HPS) resulted in the same critical Mach number for DDT.

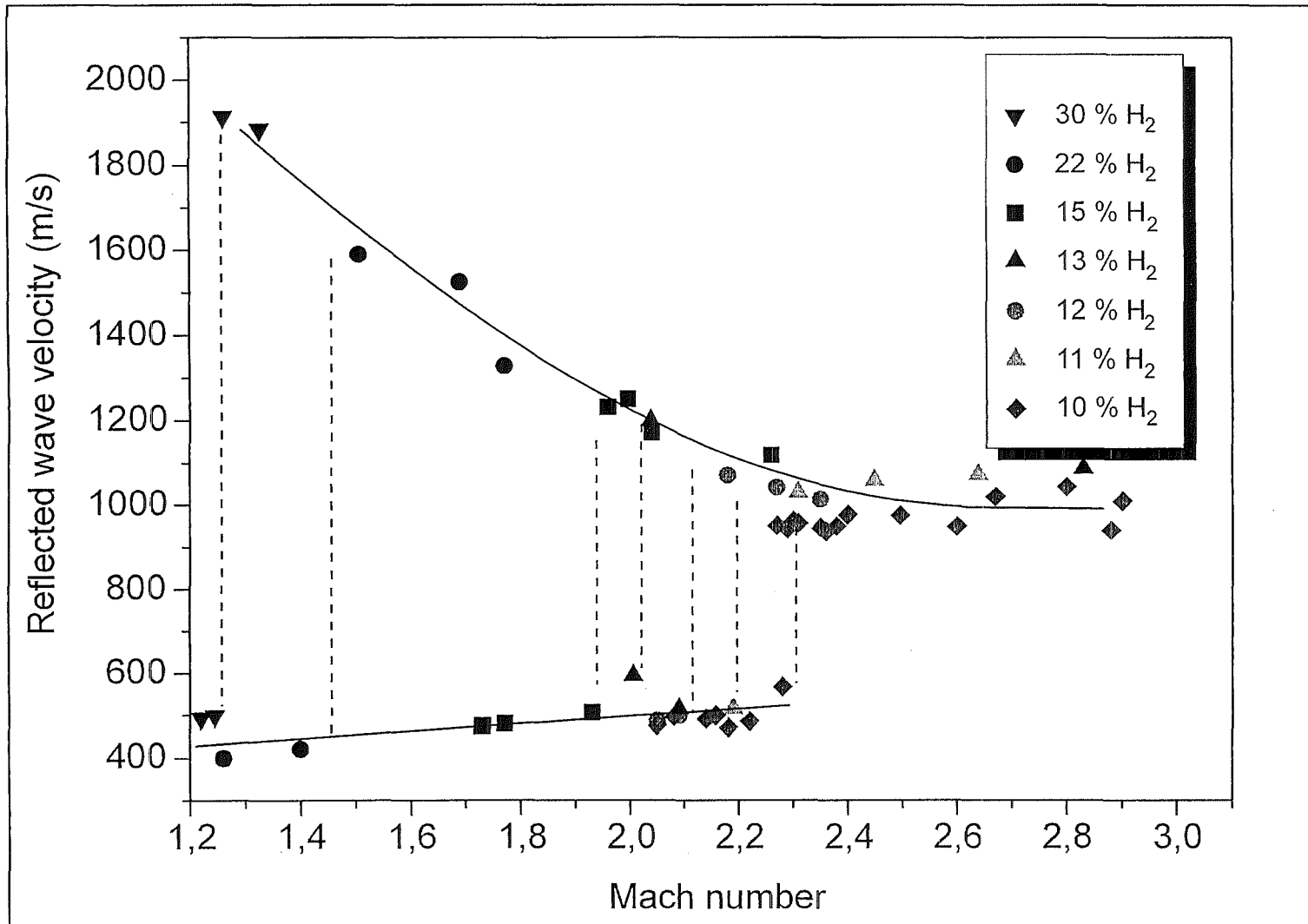


Fig. 20: Critical Mach numbers for idealised mode A- DDT in FZK- tube experiment

## 2.2. Results of prototypic mode A-DDT experiments

All experiments that were performed in the prototypic mode A arrangement are listed in Table 2. The main idea behind this experimental set-up is that after a weak spark ignition, the propagating flames reaches a highly obstructed region in which it can accelerate due to intense turbulence generation. This fast flame then emits precursor pressure waves which propagate through a relatively open region until they are reflected from the enclosure. In most practical cases the precursor wave will not simply be normally reflected from a flat wall but rather be focused by two walls (2-d wedge) or three walls (3-d corner). Such focussing geometries in industrial buildings were simulated in the tube tests by a conical reflector situated at the end of the tube, opposite to the ignition location. The investigated tube geometry contains therefore all characteristic elements of a combustion sequence in a complex industrial installation:

- a combustible gas,
- a weak ignition source,
- a partly blocked region with flow obstacles producing high turbulence levels,
- an open region which permits pressure wave propagation without significant losses, and
- a multidimensional reflector as part of the enclosure.

**Table 2:** Test matrix of DDT experiments in prototypic mode A tube configuration

Experiment	BR [%]	$p_0$ [bar]	[H <sub>2</sub> ] [%]	Obstacle separation
R0797_00	60	1	15	$\Delta x = 50\text{cm}$
R0797_01	60	1	20	$\Delta x = 50\text{cm}$
R0797_02	60	1	18	$\Delta x = 50\text{cm}$
R0797_03	60	1	17	$\Delta x = 50\text{cm}$
R0797_04	60	1	17	$\Delta x = 50\text{cm}$
R0797_05	60	1	17	$\Delta x = 50\text{cm}$
R0797_06	60	1	16	$\Delta x = 50\text{cm}$
R0797_07	60	1	16,5	$\Delta x = 50\text{cm}$
R0797_08	60	1	16,5	$\Delta x = 50\text{cm}$
R0797_09	60	1	16,5	$\Delta x = 50\text{cm}$
R0797_10	60	1	16,5	$\Delta x = 50\text{cm}$
R0797_11	60	1	16,5	$\Delta x = 50\text{cm}$
R0797_12	60	1	16,5	$\Delta x = 50\text{cm}$
R0797_13	60	1	17	$\Delta x = 50\text{cm}$
R0797_14	60	1	15	$\Delta x = 50\text{cm}$

The main results obtained in this prototypic mode A configuration will be described by two examples. Figure 21 shows the R-t-diagram of experiment R0797\_14. The test parameters of this experiment were 15.0 % hydrogen in air with an initial pressure of 1 bar. After ignition, the flame accelerated early in the obstacle section and a stable pressure /flame complex propagated in the blocked region. After

transition into the smooth part of the tube, the flame decelerates, a shock separates from the flame, and propagates towards the conical reflector.

Figure 22 shows an enlarged part of the R-t-diagram for the tube section close to the conus (9.75 m - 12.0 m). No photodiode and ionisation signals were recorded close to the incident shock, which shows that the turbulent flame has not yet reached this tube section. The measured velocity of this precursor shock wave is about 680 m/s. This precursor shock wave is focussed and reflected in the conus, but the absence of photodiode signals shows that no selfignition has taken place in the conus. The reflected wave seems to have initiated a restricted local explosion at the 10.75 m position as indicated by the short pressure excursion and the corresponding photodiode signal. The local ignition did not propagate along the tube. The sudden increase in light at the 9.75 m position (19ms) is due to the compression of burned gas because the flame arrived at this location already at about 15 ms. The average velocity of the reflected shock wave is measured to 650 m/s, which indicates that no DDT event occurred in this test.

Experiment R0797\_10, which was performed with 16.5 % hydrogen in air and an initial pressure of 1 bar led to different results. The measured R-t-diagram is shown in Figure 23. This diagram also shows an acceleration of the flame in the obstacle section and a separation of shock and flame in the smooth part of the tube. A triangular blast wave, similar to the idealised mode A test with 1m-HPS, is emitted towards the reflector.

Figure 24 is again an enlarged part of the R-t-diagram near the conus (9.75 m - 12.0 m). This time the focussed precursor shock wave causes a strong self-ignition, which is due to the higher wave speed and the more sensitive mixture. This ignition is detected simultaneously by the photodiodes, the ionisation gauges and the pressure transducers. The measured pressures are significantly higher than in the previously discussed case (Fig.22) and the values initially exceed the theoretical CJ-pressures indicating an overdriven detonation. ( $p_c/p_0 \approx 11.2$  for 16.5 %  $H_2$  in air). The flame front and the reflected shock wave remain coupled and travel with a measured velocity of 1360 m/s. Such a velocity is typical for a detonation in the counterflowing gas, indicating that a DDT event has occurred.

All experiments performed in the partly obstructed geometry can be grouped in three regimes with respect to the flame/pressure wave interaction:

- At low hydrogen concentrations ( $\leq 11\%$ ) the speed of the propagating flame in the obstructed zone remains much smaller than the sound speed in the unburned gas. The flame emits a set of acoustic waves, and the pressure increases practically uniformly in the tube according to the fraction of gas burned at any given time.
- In the second regime, which occurs for hydrogen concentrations from about 12 to 18 % (at  $p_0 = 1\text{bar}$ ,  $T_0=300\text{K}$ ) a coupled flame/shock complex is emitted from the section with obstacles. Due to the flame deceleration in the smooth part of the tube, a shock wave proceeds the flame. The shock is faster than the flame. Depending on the Mach number, the precursor wave can trigger a weak (deflagrative) or a strong (detonative) ignition when it is reflected at the tube end.

- A third regime is observed when the hydrogen concentration exceeds 18%. In this case flame and shock remain coupled after the complex leaves the obstructed region, at least for the distance available in the present test set-up. Flame and shock have the same velocity. The interaction of this complex with the tube end causes only a reflected wave back into combustion products, and contrary to regime II, no secondary ignition can occur.

DDT by mode A is only possible in the second regime where the shock velocity exceeds the flame speed. The corresponding measured range of hydrogen concentrations (12-18%) is not universal, it will generally depend on the tube dimensions and details of the obstacle section (length, blockage ratio). Experiments in a geometrically similar but scaled down facility of the Russian Academy of Science (linear scale 1:6) have identified the same three regimes but at hydrogen concentrations which were several percent higher than in the FZK-tube tests [1].

The three described regimes lead to different load mechanisms and load magnitudes. In the first case ( $v_{\text{flame}} \ll c$ ) the pressure increases nearly uniformly in the tube. The pressure increase at a given time is proportional to the fraction of burned gas at that time. Shape and size of the reflector have no influence on local pressure loads.

In the second regime ( $v_{\text{flame}} < v_{\text{shock}}$ ) two effects lead to higher loads compared to the first regime:

1. directed flow with particle velocities of the order of several 100 m/s,
2. secondary ignition after reflection in the multidimensional target at the tube end.

For low shock velocities, which only trigger a deflagration, the additional loading from the secondary ignition is not substantial. The pressure loads are comparable to that of an inert reflection. However in case of sufficiently high shock speed the strong secondary ignition causes very high local pressures because the chemical reaction proceeds from a precompressed state.

Compared to the loads in the second regime, the third regime ( $v_{\text{flame}} = v_{\text{shock}}$ ) produces lower pressures and impulses. The particle velocities of the directed flow increase, but this is more than compensated by the fact that no secondary ignition can occur from the reflection process.

In summary, the highest loads were observed inside the 3-d reflector under DDT conditions. In this case the directed flow into the conus precompressed unreacted gas which then ignited rapidly. An overdriven detonation propagates away from the reflector into the rest of the unburned gas.

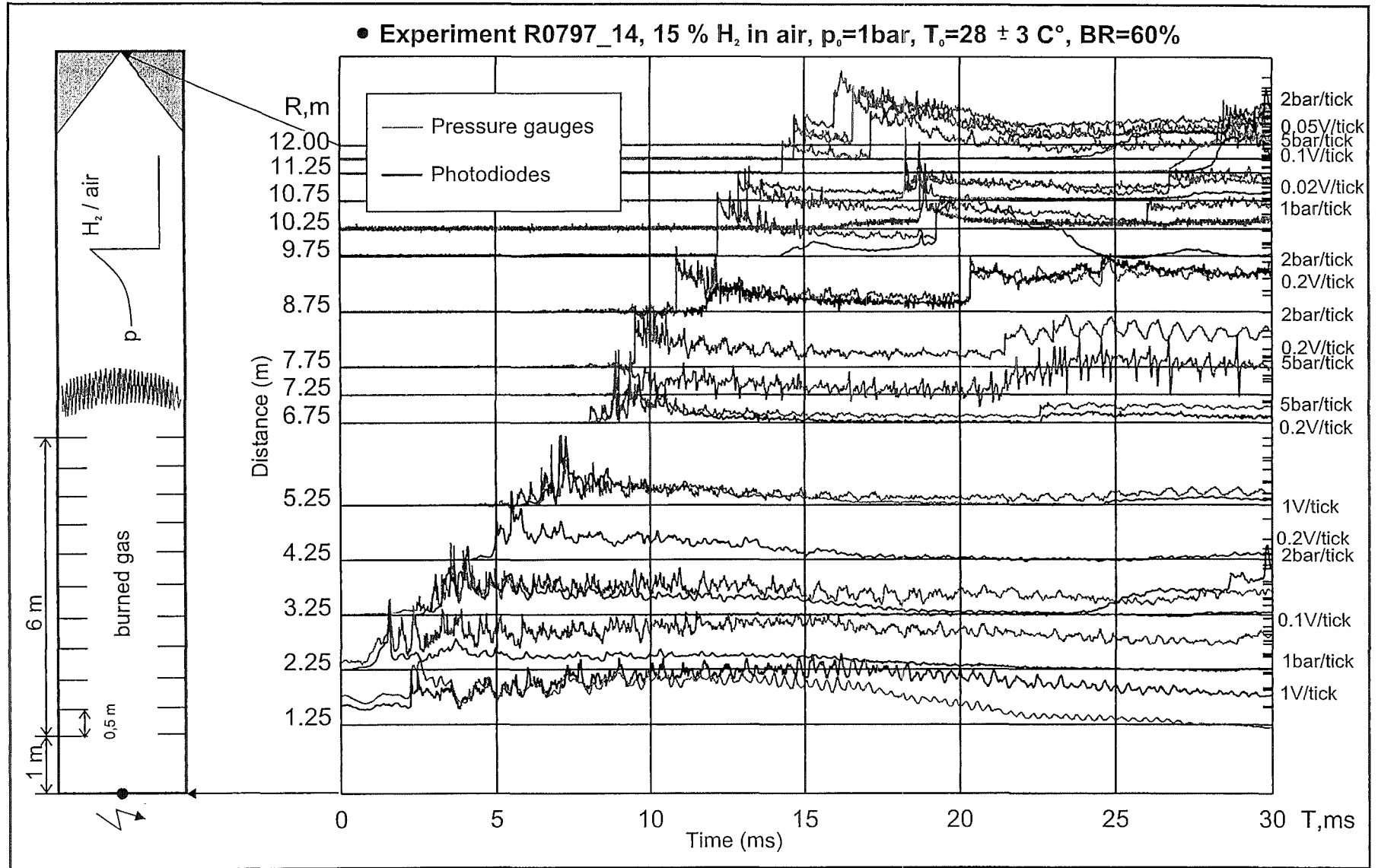


Fig. 21: Measured pressure and photodiode signals of experiment R0797\_14

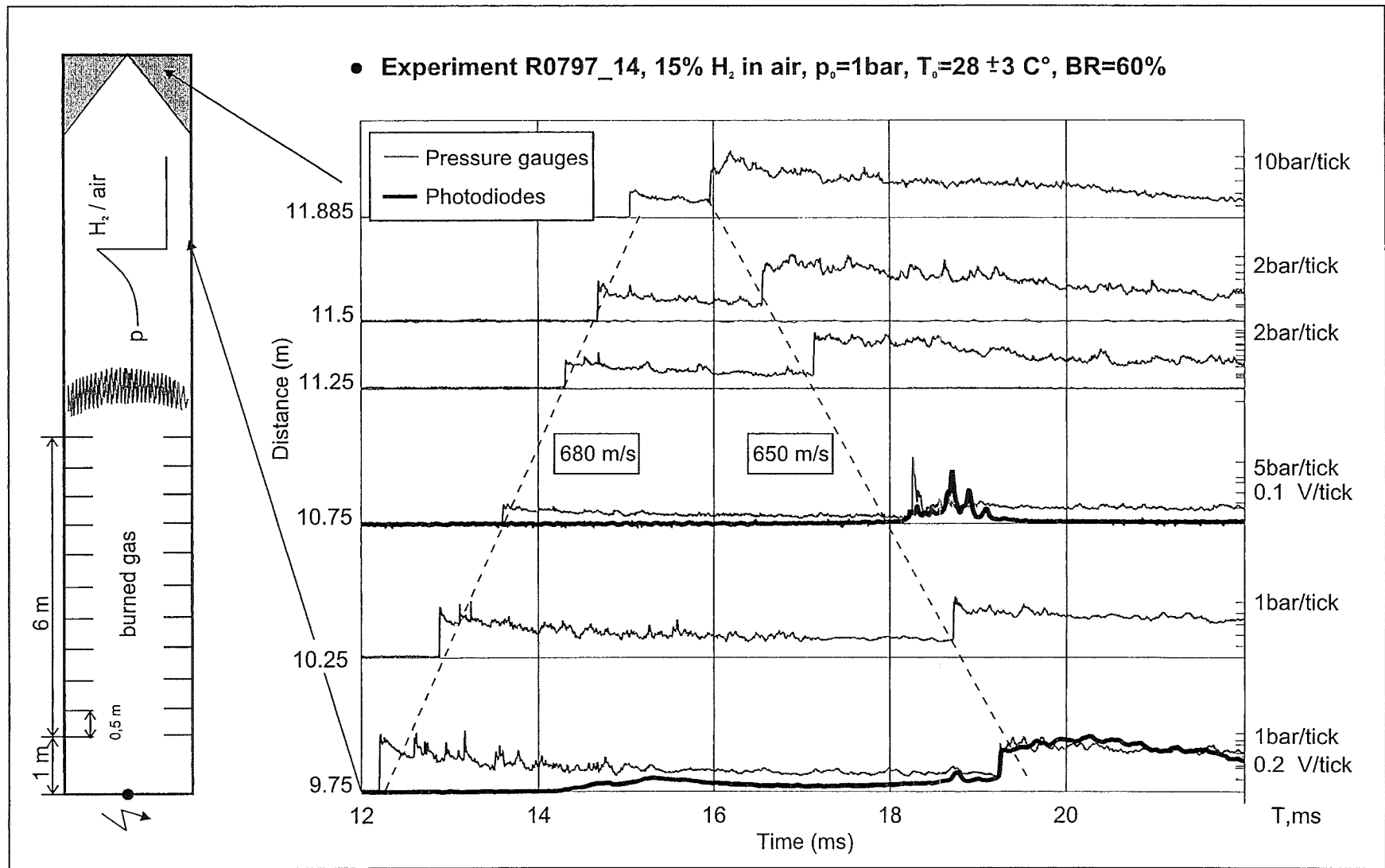


Fig. 22: Measured pressure , photodiode and ionisation signals of experiment R0797\_14. Enlarged part of the R-t diagram near the conus (9.75-12.0m)

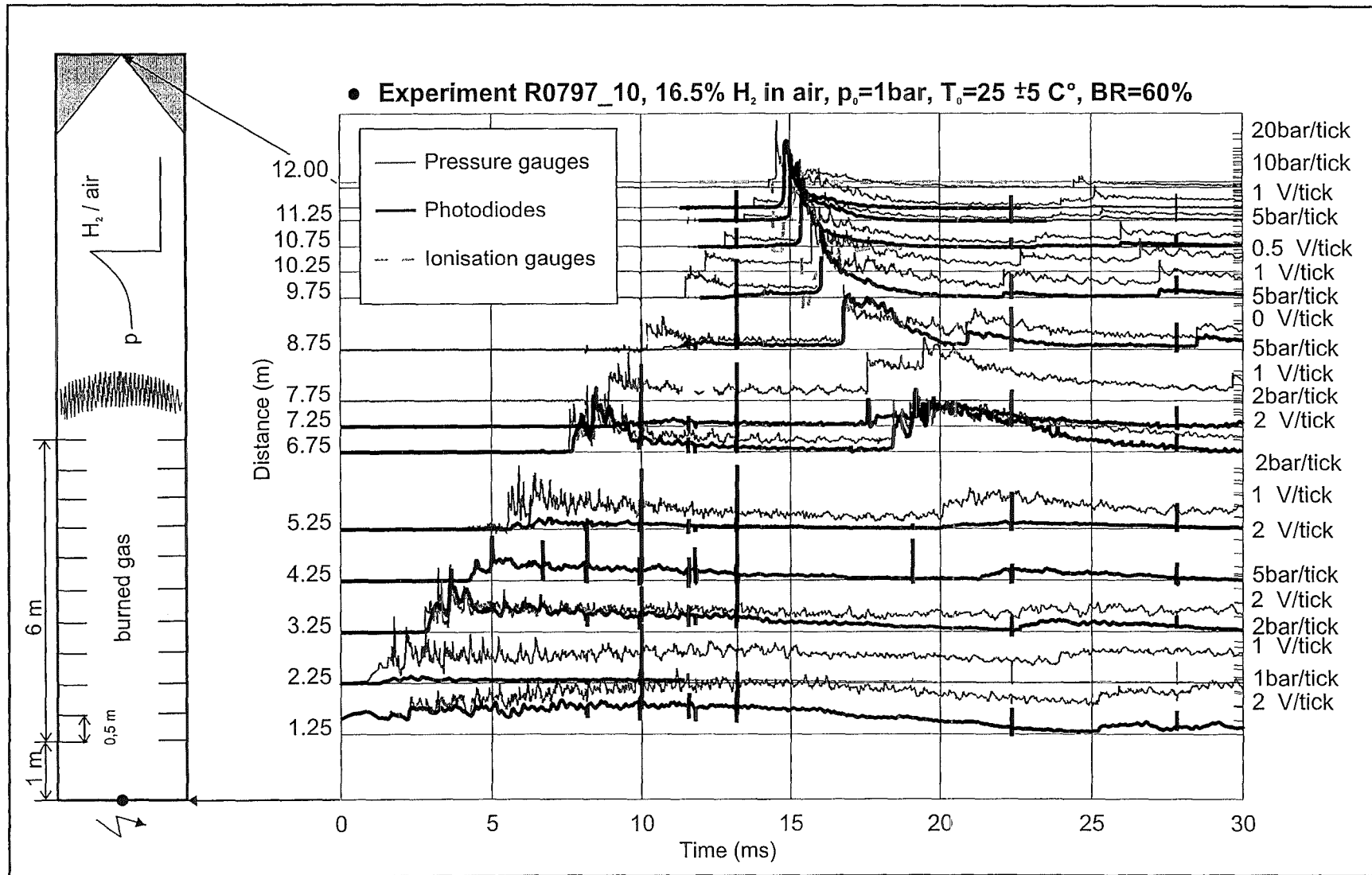


Fig. 23: Measured pressure, photodiode and ionisation signals of experiment R0797\_10.

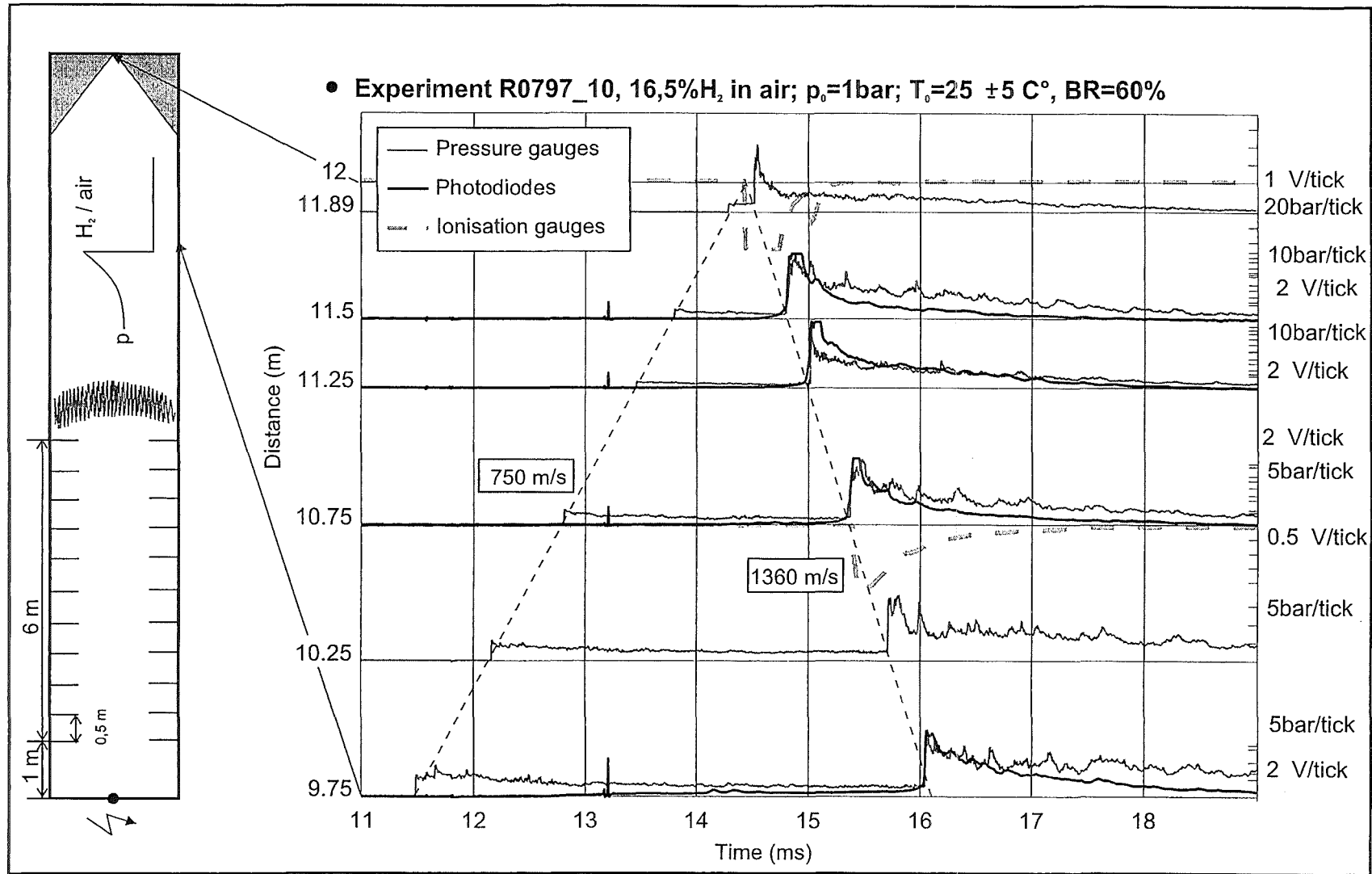


Fig.24: Measured pressure, photodiode and ionisation signals of experiments R0797\_10. Enlarged part of the R-t diagram near the conus (9.75-12.0m)

### 2.3 Results of mode B-DDT experiments

All experiments performed on mode B-DDT are listed in Table 3. The experimental parameters of the 32 tests were the hydrogen concentration (9-20 % H<sub>2</sub>) and the blockage ratio (BR=30 and 45 %). The "+" and "-" signs in the last column of the Table 3 indicate whether a DDT was observed ("+" or "-").

The measured pressure and light-signals of experiment R0498\_02, which was a typical experiment without DDT, is shown in Figure 25. This experiment was performed with a blockage ratio of 30 % and a hydrogen concentration of 11 % in air. The photodiode signals show that the flame velocity is slow in the beginning (<100 m/s). It accelerates up 450 m/s towards the end of the tube but clearly stays below the quasi-detonation velocity. The pressure signals obtained in this experiment also indicate a rather slow combustion because at first only a smooth pressure increase is observed when the flame passes the pressure transducers. The pressure level rises towards the end of the tube, but stays well below typical detonation pressures.

If this experiment is compared with experiment R0498\_13, which used a higher hydrogen concentration in air (13.5 %) but an unchanged blockage ratio, a completely different sequence of events is observed (Fig.26). In this experiment there is again an initial slow acceleration phase in which the flame front velocity reaches 250 m/s, but it then accelerates very fast up to 600 m/s (at the 5 m location), and finally reaches up to 1500 m/s (near the 8.5 m location). This velocity is close to that of a stable CJ-detonation. The pressure signals also show, after an initial acceleration phase, from 8 m on a shock-type pressure history, which is typical for a quasi-detonation. Another indication for detonation is the close coupling of the pressure and light fronts, which agreed after DDT within a few  $\mu$ s. Figures 25 and 26 were plotted on the same time scale to allow a direct visual comparison of the flame acceleration and terminal flame speed. The relatively small increase in the hydrogen concentration from 11 to 13.5% caused a reduction in the total combustion time of almost a factor of 3.

The flame trajectories of the experiments with 12, 15, 16.5 and 20 % hydrogen in air for a blockage ratio of 30 and 45 % are shown in Figure 27. The numbers in Figure 27 indicate the local flame velocity, which was determined from the arrival time of the flame between adjacent photodiodes. Note the different time scales used for different H<sub>2</sub> concentrations. The experiments with 12 % hydrogen in air show a much longer extended slow acceleration phase (0-5 m) than the experiments with a higher

**Table 3:** Experiments performed on prototypic mode B-DDT in fully obstructed combustion tube.

Experiment	BR	H <sub>2</sub> %	DDT observed
R0498_00	30	11	-
R0498_01	30	11	-
R0498_02	30	11	-
R0498_03	30	12	+
R0498_04	30	12	+
R0498_05	30	12	+
R0498_06	30	10	-
R0498_07	30	10	-
R0498_08	30	15	+
R0498_09	30	15	+
R0498_10	30	20	+
R0498_11	30	16,5	+
R0498_12	30	15	+
R0498_13	30	13,5	+
R0498_14	30	13,5	+
R0498_15	30	9	-
R0498_16	30	9	-
R0498_17	45	11	-
R0498_18	45	11	-
R0498_19	45	12	+
R0498_20	45	15	+
R0498_21	45	20	+
R0498_22	45	10	-
R0498_23	45	9	-
R0498_24	45	16,5	+
R0498_25	45	14	+
R0498_26	45	16	+
R0498_27	45	18	+
R0498_28	45	10	-
R0498_29	45	10	-
R0498_30	45	20	+
R0498_31	45	16,5	+

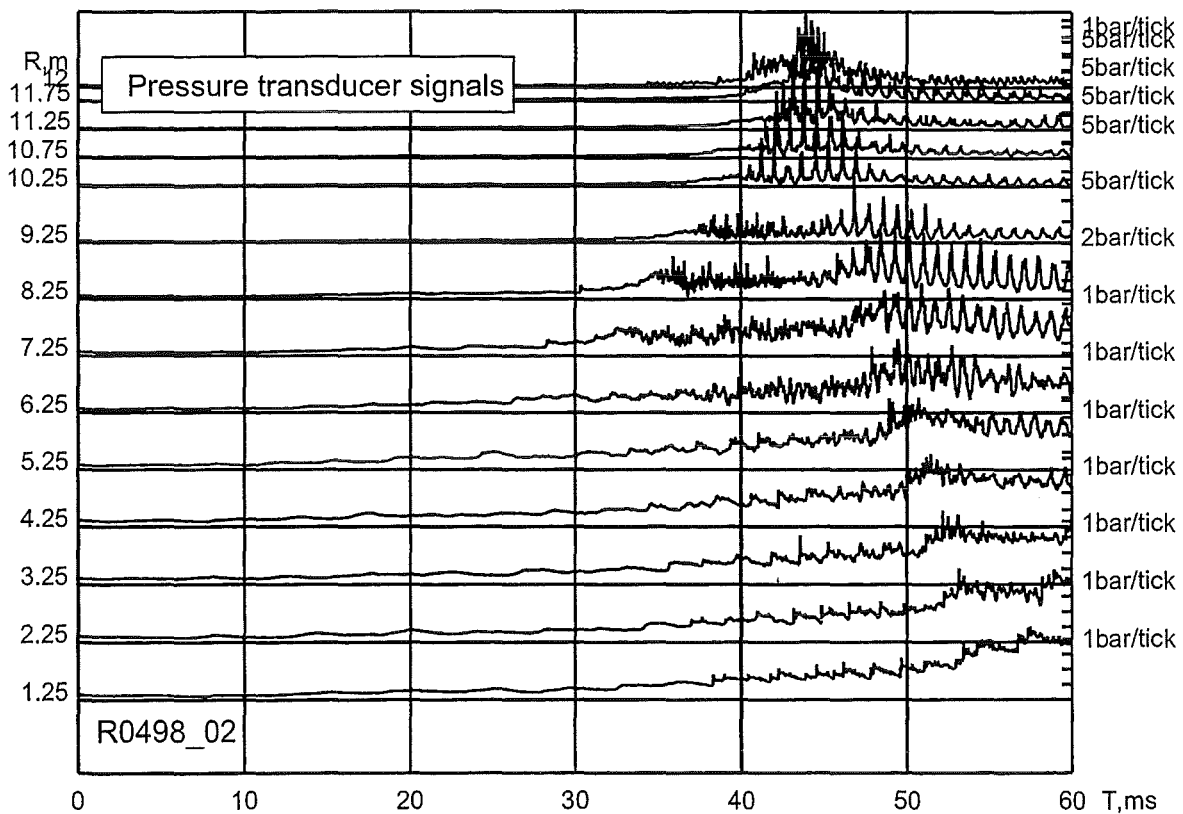
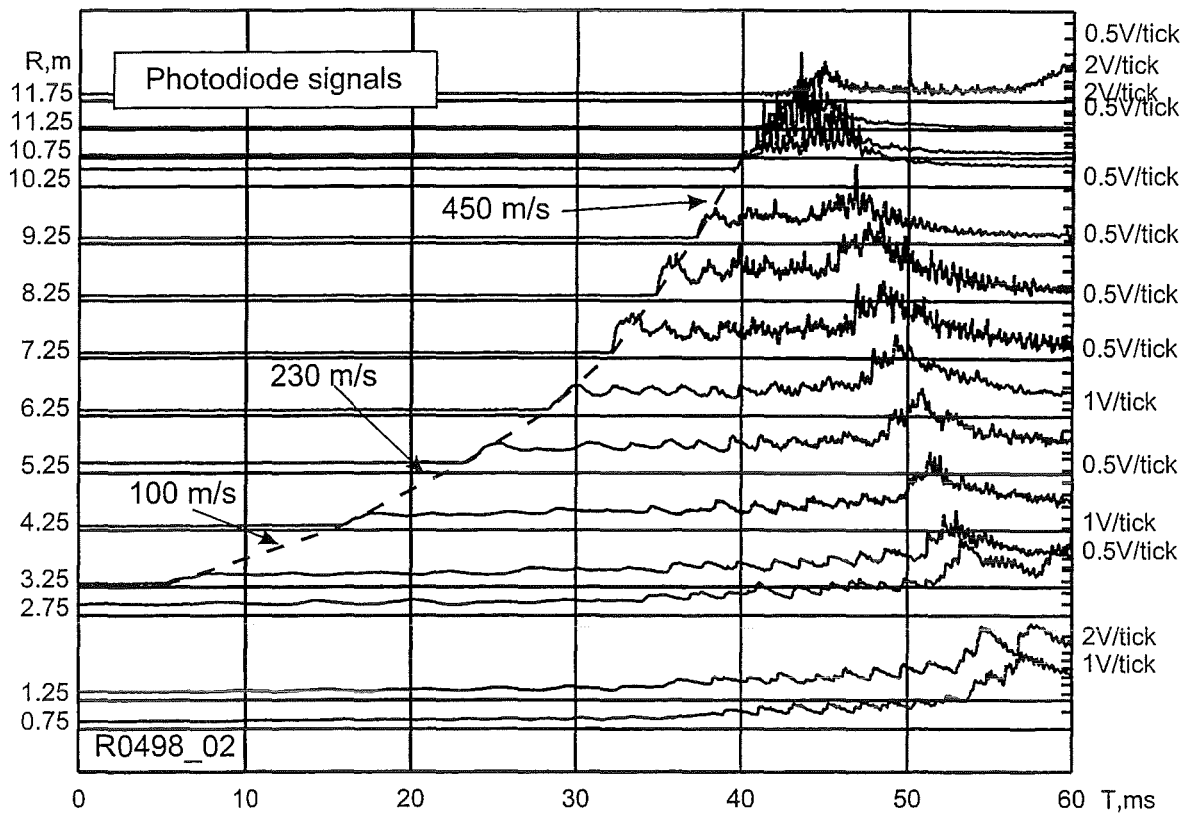


Fig. 25: Experiment on mode B-DDT. Photodiode and pressure signals show that no DDT occurred with 11 % H<sub>2</sub> in air.

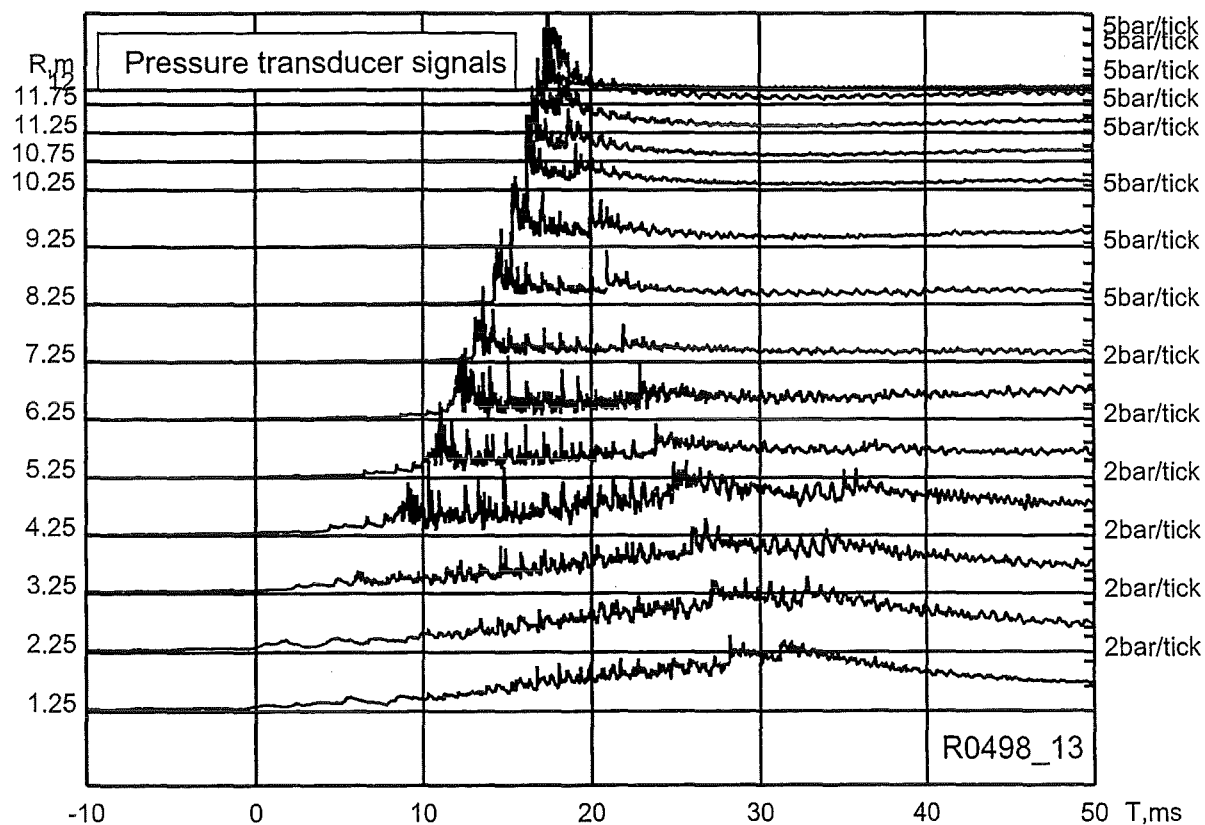
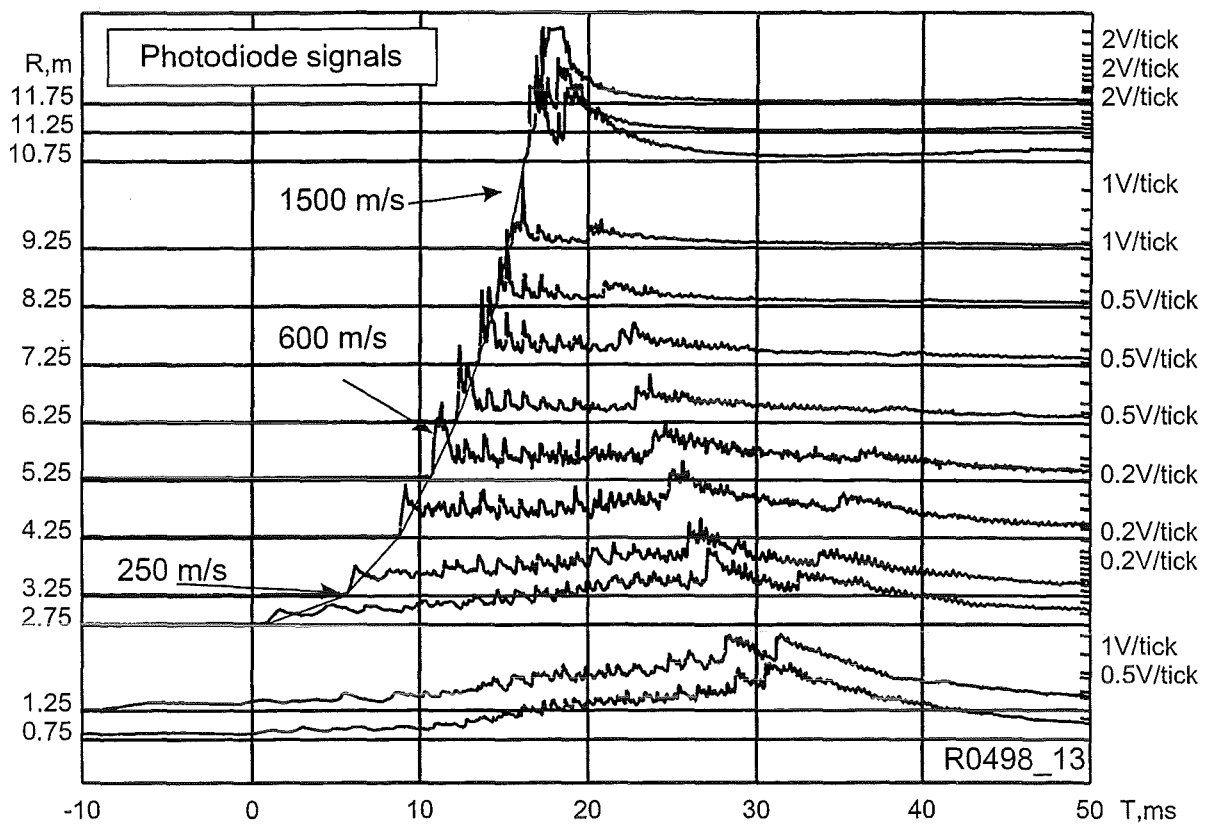


Fig. 26: Experiment on mode B-DDT. With 13.5 %  $H_2$  in air a fast flame acceleration and DDT was detected by photodiodes and pressure transducers.

hydrogen concentration (0-2.5 m). A comparison of the measured local flame velocities in experiments with different hydrogen concentrations, shows that the experiments with 12 % hydrogen reach lower maximum velocities than those with a higher hydrogen concentration. These velocities are much smaller than the theoretical CJ- detonation velocity. For 15, 16.5 and 20 % hydrogen the corresponding CJ-velocities are reached, although in different distances from the ignition point. In the present test facility DDT was observed for more than 13.5 % hydrogen in air.

In addition to the flame velocities the occurrence of DDT can be confirmed from the recorded pressure and light signals. The light and pressure signals of the experiment with 12 % (R0498\_5), shown in Figure 28, and the signals of the experiment with 16.5 % (R0498\_11) shown in Figure 29, were analysed in more detail.

A comparison of the two cases shows first of all, that the experiment with 16.5 % hydrogen reaches much higher pressures than the experiment with 12 % hydrogen (bottom part of Figures 28 and 29). Furthermore it is observable that in the experiment with 16.5 % hydrogen the flame front catches up with the shock and couples to it at a distance of about 5-6 m from the ignition point (top of Fig.29). This is also the point, where the pressure profile changes from a slowly rising combustion pressure to a shock-like detonation pressure. Also the corresponding x-t-diagram in Fig.27 (bottom,left) shows at this location a sudden acceleration from 900 m/s to 1500 m/s. This velocity remains approximately constant to the end of the tube, and corresponds to the CJ-detonation velocity. In the experiment with 12 % hydrogen no coupling of light and pressure is observed (Fig.28). The pressure profiles show a shape which is typical for a choked flow deflagration. This leads to the result, that for this kind of tube configuration a transition from deflagration to detonation can be observed and located for concentrations >13.5 % hydrogen in air. The transition locations were found for 15 % hydrogen at 7m , for 16.5 % hydrogen at 6 m, and for 20 % hydrogen at 3.5 m from the point of ignition.

Comparison of the experiments with a different BR but constant hydrogen concentration shows the same point of transition for 16.5 and 20% H<sub>2</sub>, however the maximum velocities of the experiments with 30 % BR are slightly higher than with 45 % BR. At 15% hydrogen DDT occurred with 30% BR, but not with 45% BR. A longer tube may have permitted DDT also with 45% BR. Compared to the 30 % BR, the increase to 45 % BR produces a faster initial flame acceleration (more turbulence) but on the other hand only permits lower terminal flame speeds (increased flow resistance).



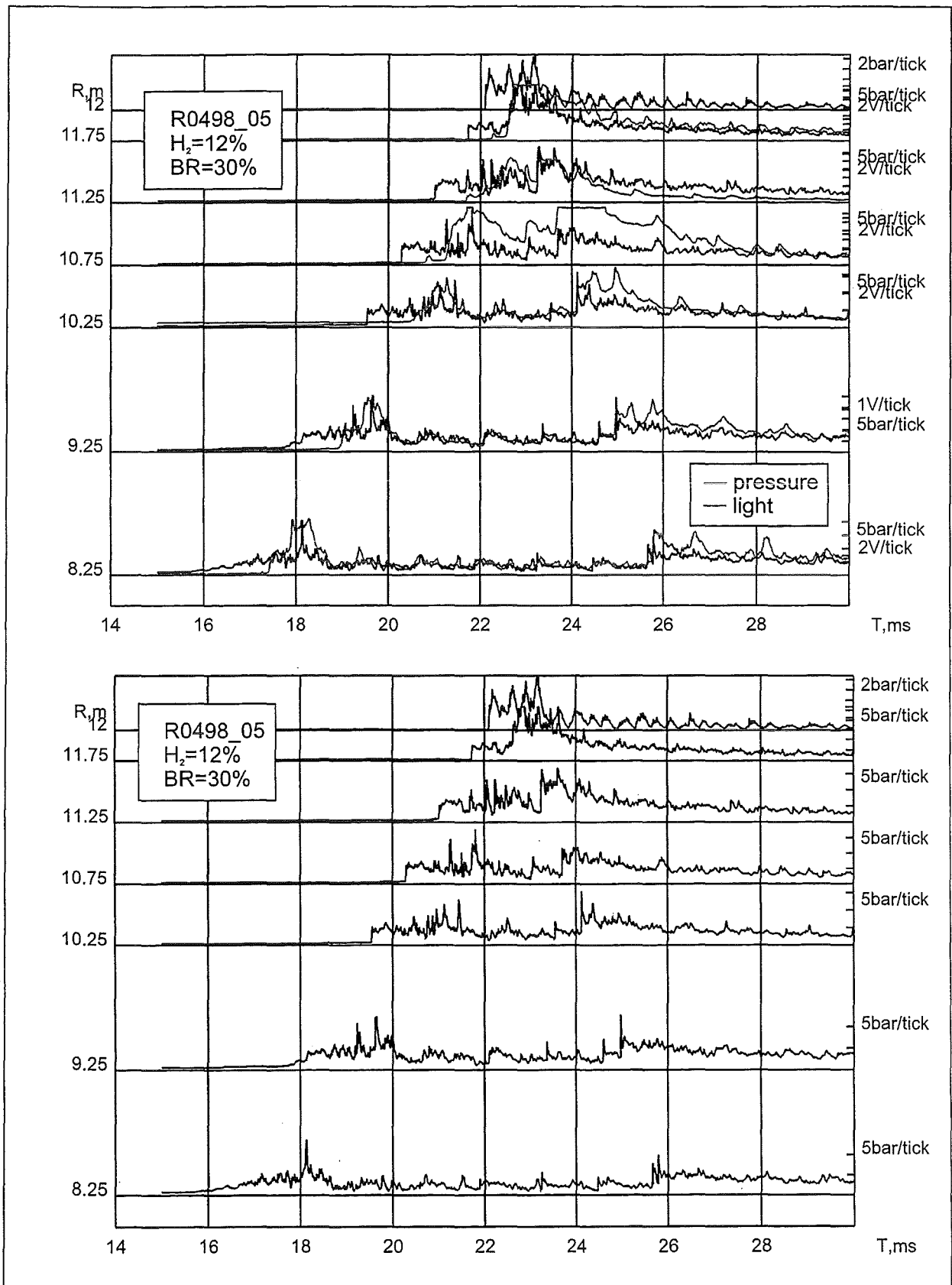


**Fig.28:** Pressure and light signals in case of an experiment without DDT. Top: no coupling of pressure and flame front. Bottom: deflagration type pressure amplitudes and profiles.

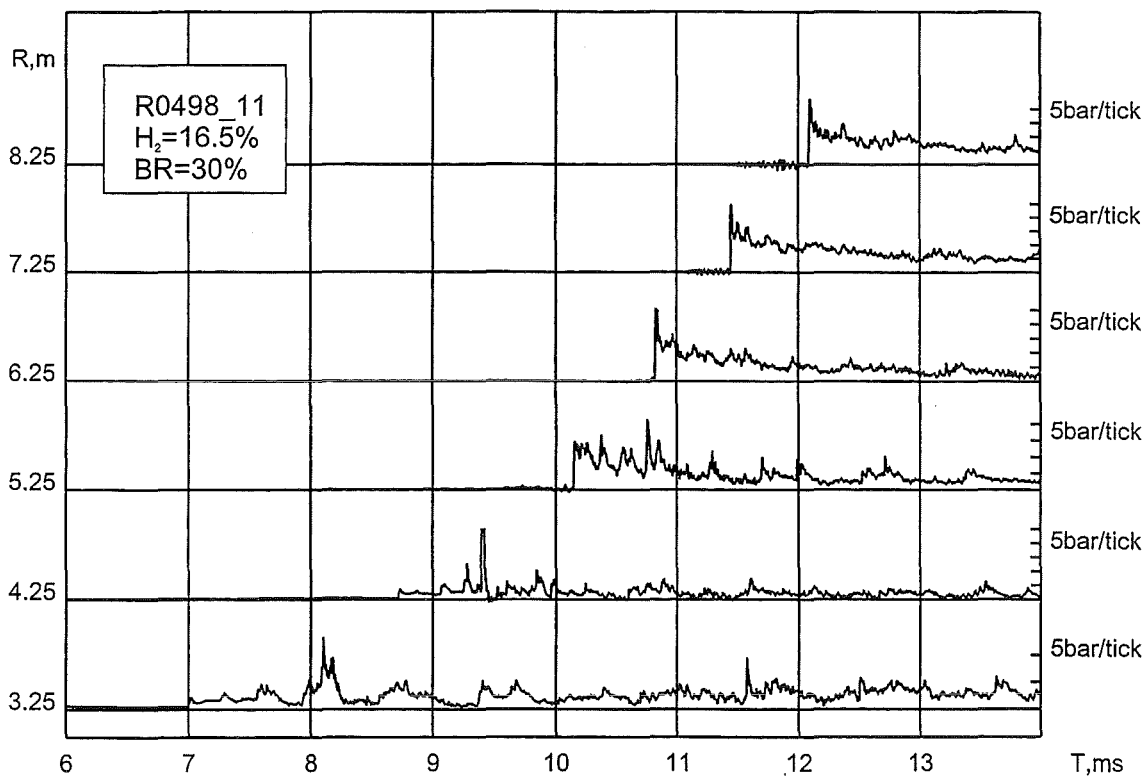
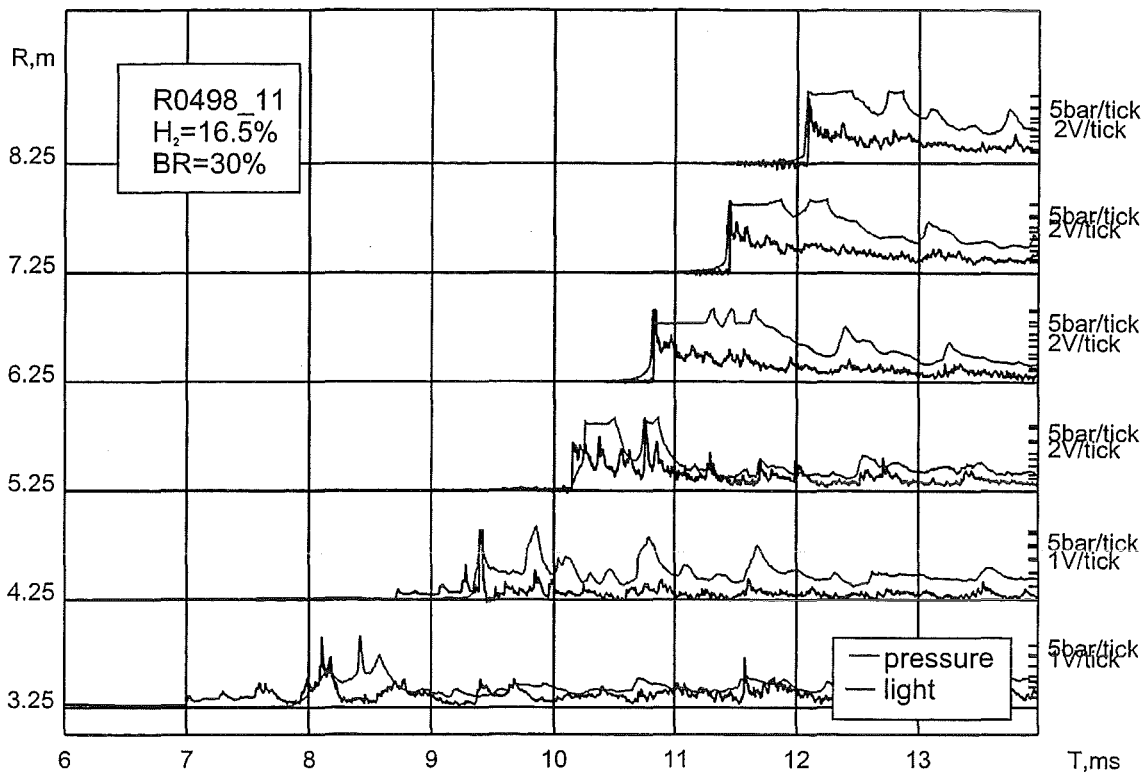


**Fig.29:** Pressure and light signals in case of an experiment with DDT by mode B. Top: coupling of shock and flame front between the 5 and 6 m positions. Bottom: change from deflagration-like to detonation like pressure amplitudes and shapes.

### 3. Numerical simulation of DDT

Although it is currently difficult to simulate the described experiment in full 3-d geometry, a simplified 2-d calculation can reproduce the observed sequence of events and illustrate the complex interaction between flow and chemistry which then leads to a fully developed detonation.

A 2-d section of the shock tube (idealized mode A experiment) was simulated in a test calculation with a spatial resolution of 2 mm (grid =  $88 \times 600 \times 2 \approx 10^5$  cells). The LPS of the shock tube was initially filled with stoichiometric  $H_2$ -air mixture at 1 bar and 298 K. The HPS contained helium at 10 bar. These initial conditions lead to a shock Mach number of  $Ma = 1.39$ . The  $H_2$ - $O_2$  reaction was described with a one-step Arrhenius reaction rate which was verified in earlier detonation simulations ( $\Delta H/R = 8635$  K). Only the Euler equations were solved in this test calculation.

Fig. 30 depicts the calculated 2-d pressure field at different times in the lower half of the tube. Frame a) shows the incident shock wave, which has a peak pressure of 2.17 bar. In frames b), c) and d) the shock wave enters the reflector, the peak pressure in the reflected wave increases to 4.8 bar. In frame e) a local reaction was ignited in a pre-compressed hot spot near the end wall, driving the pressure up to 32.7 bar. Note that at this time the reflected pressure wave moving to the left already leaves the conus. The gas in this region between local ignition and leading pressure front is pre-compressed, pre-heated, and rapidly reacting after ignition by the local explosion because the induction time in this pre-conditioned mixture has already partly elapsed. Only 56  $\mu s$  later (in frame f) the local explosion has expanded sufficiently to merge with the precursor pressure wave into a stable detonation front, which then propagates to the left (frames g, h, i). The calculated detonation speed is approx. 2000 m/s and close to the Chapman-Jouguet detonation velocity of the undisturbed mixture.

The calculated pressures and wave velocities indicate that the gasdynamic compression leads to a strong local ignition and explosion near the focus of the conus, an initially overdriven detonation kernel which rapidly amplifies in locally pre-conditioned gas, and then relaxes towards the CJ-conditions of the shocked gas, as it moves out of the conus back into the tube section. A similar calculation with a lower initial pressure in the high pressure section (3 bar) showed no ignition in the conus. In summary, the test calculations with simplified geometry (2d) and chemistry (1 step Arrhenius) have qualitatively reproduced all essential phenomena observed in the DDT experiments, indicating that the theoretical model contains the governing physical processes.

In the above described case a shock wave was used to produce local hot spots in a multidimensional reflector. The prototypic-mode-A tests in the FZK tube showed that precursor pressure waves from fast flames (e.g. at 16 %  $H_2$  in air) are also able to produce strong local hot spots and a transition into a stable detonation.

With respect to numerical simulation it is necessary to discriminate DDT on reflection from the more complicated case of DDT near a turbulent flame brush.

In the first case (discussed above) the mixture is predefined and also no turbulence simulation is necessary. Today's CFD tools allow to reproduce DDT in reflection in small scale 3d geometries or in medium-scale 2d configurations. Adaptive mesh

refinement allows to show grid independence of the results. It appears that simple one- or few-step chemistry models are sufficient to reproduce the occurrence and timing of the local explosion and the succeeding detonation propagation.

Simulation of DDT in or near a turbulent flame brush is a much more complicated problem which still requires substantial development in theoretical models, numerical techniques and computational resources for the following reasons:

- the importance of turbulence and the required model representation is not yet clear,
- the preparation of the reactive medium by mixing of burned gas (radicals) with unburned gas components ( $O_2$ ,  $H_2$ ) is very complicated,
- the ignition seems to have some stochastic character,
- the formulation of an adequate chemistry model needs to be investigated in detail,
- a very high spatial resolution is required for modelling of chemistry and turbulence.

Mechanistic model development and successful validation of numerical tools for this type of DDT events is therefore still far in the future.

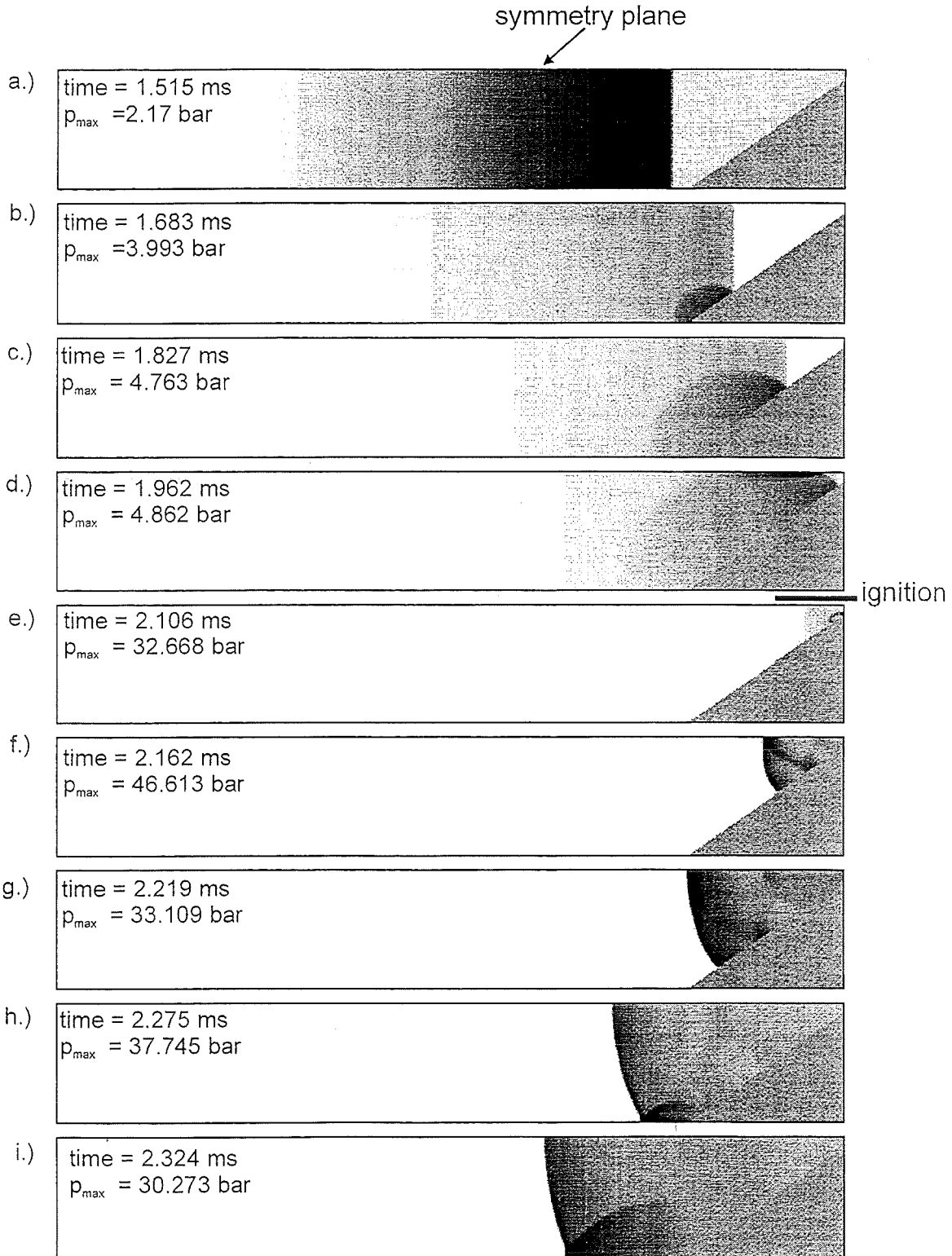


**Fig.30** Numerical simulation of shock induced hot spot formation in a 2-d reflector, local explosion, and transition into a stable detonation (stoichiometric  $\text{H}_2$ -air,  $p_0 = 1$  bar,  $T_0 = 298$  K,  $M_{\text{Shock}} = 1.39$ ). Ignition of the pre-compressed mixture occurs between frame c) (4.8 bar) and frame e) (32.7 bar).

## References

- [1] J.W. Yang, Z. Musicki, S. Nimnual, "Hydrogen Combustion Control and Value Impact Analysis for PWR Dry Containments", NUREG/CR-5662 (June 1991).
- [2] J. Rohde, GRS, private communication, 1997
- [3] G. Katzenmeier, H.U. Hahn, T. Cron (eds), (Techn. Fachbericht )PHDR (March 1994).
- [4] M.P. Sherman, M. Berman, "The Possibility of Local Detonations During Degraded- Core Accidents in the Bellefonte NPP" Nuclear Technology Vol. 81 (April 1988), p.63.
- [5] B.E. Gelfand, S.V. Khomik, A.M. Bartenev, S.P. Medvedev, H.Groenig, "Detonation initiation at the focusing of shock waves in combustible gaseous mixture", 17<sup>th</sup> International Colloquium on the Dynamics of Explosions and Reactive Systems (ICDERS), July 25-30, 1999, Heidelberg, Germany
- [6] W. Breitung, C. Chan, S. Dorofeev, A. Eder, B. Gelfand, M. Heitsch, R. Klein, A. Malliakos, E. Sheperd, E. Studer, P. Thibault , "State-of-the-Art Report on Flame Acceleration and Deflagration-to Detonation Transition in Nuclear Safety", OECD/NEA Report, (1999) in print.
- [7] B.E. Gelfand, S.V. Khomik , "Investigation of Hydrogen and Air Fast Flame Propagation and DDT in Tube with Multidimensional Endplates", Final Report to FZK, Russian Academy of Sciences, Moscow 1997
- [8] B.E. Gelfand, S.V. Khomik , A.N. Polenov , "DDT Experiments with Focusing of H<sub>2</sub> and Air Blast Waves", Final Report to FZK, Russian Academy of Sciences, Moscow 1997

## Acknowledgement

An important part of the idealized mode A-DDT experiments was performed jointly with Prof. B. Gelfand and his co-workers during a stay in May 1998. Their experimental and theoretical contributions are highly appreciated.